Hyperbolic Systems of Conservation Laws

in One Space Dimension

Alberto Bressan
S.I.S.S.A., Trieste 34014, Italy.

This is a survey paper, written in the occasion of an invited talk given by the author at the Universidad Complutense in Madrid, October 1998. Its purpose is to provide an account of some recent advances in the mathematical theory of hyperbolic systems of conservation laws in one space dimension. After a brief review of basic concepts, we describe in detail the method of wave-front tracking approximation and present some of the recent results on uniqueness and stability of entropy weak solutions. The last two chapters contain a discussion of the Glimm scheme, and some counterexamples to global existence and continuous dependence, in the case of large data or when the strict hyperbolicity fails. The paper has been revised in 2001, to make it suitable for use as lecture notes in a summer school.

1 - Review of basic theory.

This chapter reviews the basic definitions and properties of systems of conservation laws. For a comprehensive introduction to the theory of hyperbolic systems we refer to [5, 15, 27, 28]. In particular, all the recent results on uniqueness and stability of entropy weak solutions are covered in [5], where the reader can also find complete proofs of the theorems here stated in Sections 1–4.

1.1 - Basic definitions. A single conservation law in one space dimension is a first order partial differential equation of the form

$$u_t + f(u)_x = 0. \tag{1.1}$$

Here u is the *conserved quantity* while f is the *flux*. Integrating (1.1) over the interval $[a, b]$ one obtains

$$\begin{aligned} \frac{d}{dt}\int_a^b u(t,x)\ dx &= \int_a^b u_t(t,x)\ dx \\ &= -\int_a^b f\big(u(t,x)\big)_x\ dx \\ &= f\big(u(t,a)\big) - f\big(u(t,b)\big) \\ &= \ [\text{inflow at } a] - \ [\text{outflow at } b] \end{aligned} \tag{1.2}$$

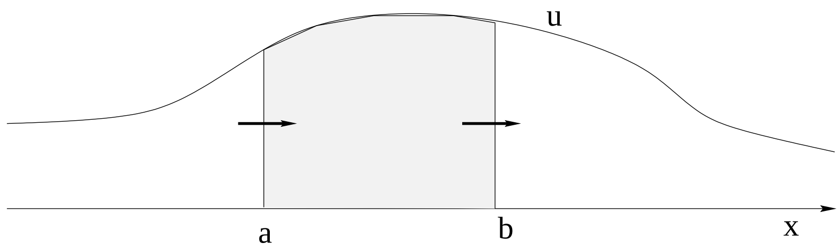

figure 1

In other words (fig. 1), the quantity u is neither created nor destroyed: the total amount of u contained inside any given interval $[a, b]$ can change only due to flow of u across the two endpoints.

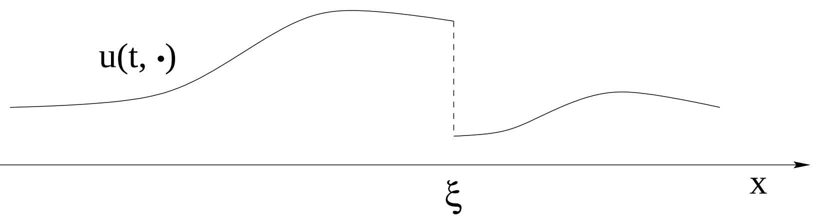

figure 2

Using the chain rule, (1.1) can be written in the quasilinear form

$$u_t + a(u)u_x = 0, \tag{1.3}$$

where $a = f'$ is the derivative of f. For smooth solutions, the two equations (1.1) and (1.3) are entirely equivalent. However, if u has a jump at a point ξ (fig. 2), the left hand side of (1.3) will contain the product of a discontinuous function $a(u)$ with the distributional derivative u_x, which in this case contains a Dirac mass at the point ξ. In general, such a product is not well defined. Hence (1.3) is meaningful only within a class of continuous functions. On the other hand, working with the equation in divergence form (1.1) allows us to consider discontinuous solutions as well, interpreted in distributional sense. More precisely, a locally integrable function $u = u(t,x)$ is a *weak solution* of (1.1) provided that

$$\int\!\!\int \big\{u\phi_t + f(u)\phi_x\big\}\, dxdt \;=\; 0 \tag{1.4}$$

for every differentiable function with compact support $\phi \in \mathcal{C}^1_c$.

The main object of our study will be the $n \times n$ *system of conservation laws*

$$\begin{cases} \dfrac{\partial}{\partial t}u_1 + \dfrac{\partial}{\partial x}\big[f_1(u_1,\ldots,u_n)\big] = 0, \\ \qquad\qquad \cdot \quad \cdot \quad \cdot \\ \dfrac{\partial}{\partial t}u_n + \dfrac{\partial}{\partial x}\big[f_n(u_1,\ldots,u_n)\big] = 0. \end{cases} \tag{1.5}$$

For simplicity, this will still be written in the form (1.1), but keeping in mind that now $u = (u_1,\ldots,u_n)$ is a vector in $I\!R^n$ and that $f = (f_1,\ldots,f_n)$ is a map from $I\!R^n$ into itself. Calling $A(u) \doteq Df(u)$ the $n \times n$ Jacobian matrix of the map f at the point u, the system (1.5) can be written in the quasilinear form

$$u_t + A(u)u_x = 0. \tag{1.6}$$

We say that the above system is *strictly hyperbolic* if every matrix $A(u)$ has n real, distinct eigenvalues, say $\lambda_1(u) < \cdots < \lambda_n(u)$. In this case, one can find dual bases of left and right eigenvectors of $A(u)$, denoted by $l_1(u),\ldots,l_n(u)$ and $r_1(u),\ldots,r_n(u)$, with

$$l_i(u)\cdot r_j(u) = \begin{cases} 1 & \text{if} \quad i = j, \\ 0 & \text{if} \quad i \neq j. \end{cases}$$

Example 1 (Gas Dynamics). The Euler equations describing the evolution of a non viscous gas take the form

$$\begin{cases} \rho_t + (\rho v)_x = 0 & \text{(conservation of mass)} \\ (\rho v)_t + (\rho v^2 + p)_x = 0 & \text{(conservation of momentum)} \\ (\rho E)_t + (\rho E v + p v)_x = 0 & \text{(conservation of energy)} \end{cases}$$

Here ρ is the mass density, v is the velocity while $E = e + v^2/2$ is the energy density per unit mass. The system is closed by a *constitutive relation* of the form $p = p(\rho, e)$, giving the pressure as a function of the density and the internal energy. The particular form of p depends on the gas under consideration.

1.2 - Linear systems. We consider here two elementary cases where the solution of the Cauchy problem can be written explicitly.

The linear homogeneous scalar Cauchy problem with constant coefficients has the form

$$u_t + \lambda u_x = 0, \qquad\qquad u(0,x) = \bar u(x), \tag{1.7}$$

with $\lambda \in I\!R$. If $\bar u \in \mathcal{C}^1$, one easily checks that the travelling wave

$$u(t,x) = \bar u(x - \lambda t) \tag{1.8}$$

provides a classical solution to (1.7). In the case where the initial condition $\bar u$ is not differentiable and we only have $\bar u \in \mathbf{L}^1_{loc}$, the function u defined by (1.8) can still be interpreted as a solution, in distributional sense.

Next, consider the homogeneous system with constant coefficients

$$u_t + Au_x = 0, \qquad\qquad u(0,x) = \bar u(x), \tag{1.9}$$

where A is a $n \times n$ hyperbolic matrix, with real eigenvalues $\lambda_1 < \cdots < \lambda_n$ and right and left eigenvectors $r_i,\ l_i$, chosen so that

$$l_i \cdot r_j = \begin{cases} 1 & \text{if} \quad i = j, \\ 0 & \text{if} \quad i \neq j, \end{cases}$$

Call $u_i \doteq l_i \cdot u$ the coordinates of a vector $u \in I\!R^n$ w.r.t. the basis of right eigenvectors $\{r_1, \cdots, r_n\}$. Multiplying (1.9) on the left by $l_1, \ldots, l_n$ we obtain

$$(u_i)_t + \lambda_i (u_i)_x = (l_i u)_t + \lambda_i (l_i u)_x = l_i u_t + l_i A u_x = 0, \qquad\qquad u_i(0,x) = l_i \bar u(x) \doteq \bar u_i(x).$$

Therefore, (1.9) decouples into n scalar Cauchy problems, which can be solved separately in the same way as (1.7). The function

$$u(t,x) = \sum_{i=1}^n \bar u_i(x - \lambda_i t)\, r_i \tag{1.10}$$

now provides the explicit solution to (1.9), because

$$u_t(t,x) = \sum_{i=1}^n -\lambda_i \big(l_i \cdot \bar u_x(x - \lambda_i t)\big) r_i = -Au_x(t,x).$$

Observe that in the scalar case (1.7) the initial profile is shifted with constant speed λ. For the system (1.9), the initial profile is decomposed as a sum of n waves, each travelling with one of the characteristic speeds $\lambda_1, \ldots, \lambda_n$.

As a special case, consider the Riemann initial data

$$\bar{u}(x) = \begin{cases} u^- & \text{if} \quad x < 0, \\ u^+ & \text{if} \quad x > 0. \end{cases}$$

The corresponding solution (1.10) can then be obtained as follows.

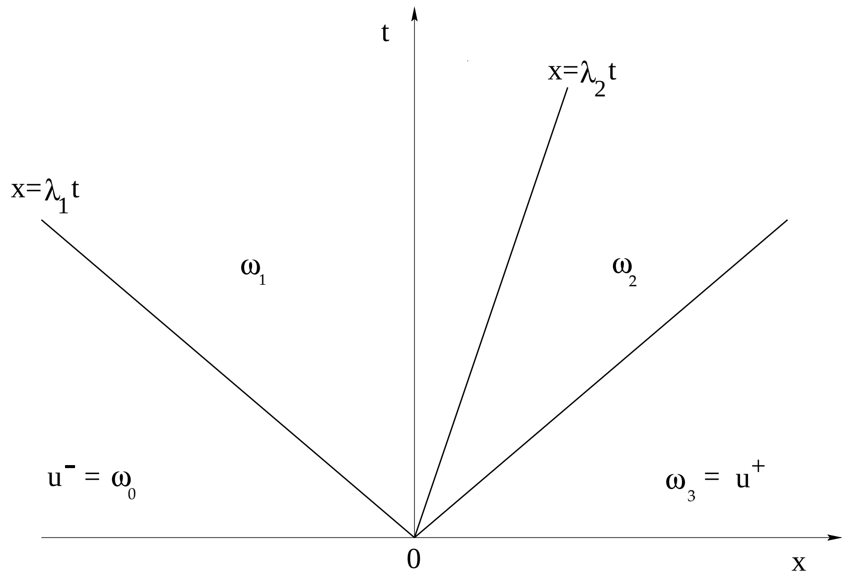

figure 3

Write the vector $u^+ - u^-$ as a linear combination of eigenvectors of A, i.e.

$$u^+ - u^- = \sum_{j=1}^{n} c_j r_j .$$

Define the intermediate states

$$\omega_i \doteq u^- + \sum_{j \le i} c_j r_j , \qquad\qquad i = 0, \ldots, n,$$

so that each difference $\omega_i - \omega_{i-1}$ is an i-eigenvector of A. The solution then takes the form (fig. 3):

$$u(t,x) = \begin{cases} \omega_0 = u^- & \text{for} \quad x/t \ < \lambda_1, \\ & \ldots \\ \omega_i & \text{for} \quad \lambda_i < x/t < \lambda_{i+1}, \\ & \ldots \\ \omega_n = u^+ & \text{for} \quad x/t \ > \lambda_n . \end{cases} \tag{1.11}$$

1.3 - Loss of regularity. A basic feature of nonlinear systems of the form (1.1) is that, even for smooth initial data, the solution of the Cauchy problem may develop discontinuities in finite time [16]. To achieve a global existence result, it is thus essential to work within a class of discontinuous functions, interpreting the equations (1.1) in their distributional sense (1.4).

Example 2. Consider the scalar conservation law (inviscid Burgers' equation)

$$u_t + \left(\frac{u^2}{2}\right)_x = 0 \tag{1.12}$$

with initial condition

$$u(0,x) = \bar{u}(x) = \frac{1}{1+x^2}\,.$$

For $t > 0$ small the solution can be found by the method of characteristics. Indeed, if u is smooth, (1.12) is equivalent to

$$u_t + uu_x = 0. \tag{1.13}$$

By (1.13) the directional derivative of the function $u = u(t,x)$ along the vector $(1,u)$ vanishes. Therefore, u must be constant along the characteristic lines in the t-x plane:

$$t \mapsto \big(t,\ x + t\bar{u}(x)\big) = \left(t,\ x + \frac{t}{1+x^2}\right).$$

For $t < T \doteq 8/\sqrt{27}$, these lines do not intersect (fig. 4). The solution to our Cauchy problem is thus given implicitly by

$$u\left(t,\ x + \frac{t}{1+x^2}\right) = \frac{1}{1+x^2}\,. \tag{1.14}$$

On the other hand, when $t > 8/\sqrt{27}$, the characteristic lines start to intersect. As a result, the map

$$x \mapsto x + \frac{t}{1+x^2}$$

is not one-to-one and (1.14) no longer defines a single valued solution of our Cauchy problem.

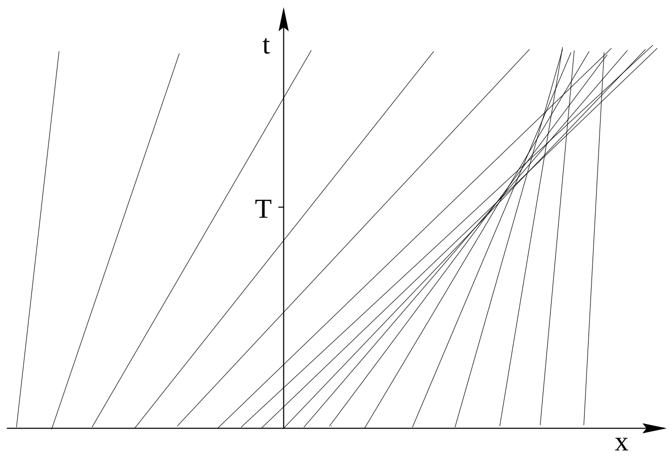

figure 4

An alternative point of view is the following (fig. 5). As time increases, points on the graph of $u(t,\cdot)$ move horizontally with speed u, equal to their distance from the x-axis. This determines a change in the profile of the solution. As t approaches the critical time $T \doteq 8/\sqrt{27}$, one has

$$\lim_{t\to T-} \left\{ \inf_{x\in I\!R} u_x(t,x) \right\} = -\infty,$$

and no classical solution exists beyond time T. The solution can be prolonged for all times $t \geq 0$ only within a class discontinuous functions.

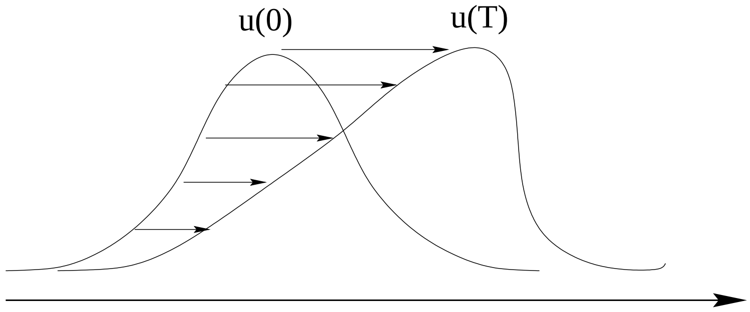

figure 5

1.4 - Rankine-Hugoniot Equations. Motivated by the previous example, for a nonlinear system of conservation laws the global solutions must be studied in a space of discontinuous functions. From now on, by a *weak solution* of the system (1.1) we mean a function $u : [0,T] \times I\!R \mapsto I\!R^n$ such that the mapping $t \mapsto u(t,\cdot)$ is continuous with values in $\mathbf{L}^1_{\rm loc}$ and such that

$$\iint \big\{ u\phi_t + f(u)\phi_x \big\}\, dxdt = 0 \tag{1.15}$$

for every differentiable function with compact support $\phi \in \mathcal{C}^1_c$ which vanishes for $t \notin [0,T]$.

Now consider a sequence of weak solutions of (1.1), converging to u in $\mathbf{L}^1_{\rm loc}\big([0,T]\times I\!R\big)$. If the u_ν are uniformly bounded, the convergence $f(u_\nu) \to f(u)$ also holds. Hence, for every $\phi \in \mathcal{C}^1_c$,

$$\iint \big\{ u\phi_t + f(u)\phi_x \big\}\, dxdt = \lim_{\nu\to\infty} \iint \big\{ u_\nu\phi_t + f(u_\nu)\phi_x \big\}\, dxdt = 0 \tag{1.16}$$

This shows that the set of weak solutions is closed under convergence in $\mathbf{L}^1_{\rm loc}$.

We now derive conditions imposed by (1.15) on a solution at points of jump. We first study the simple case of a piecewise constant solution:

$$U(t,x) = \begin{cases} u^+ & \text{if} \quad x > \lambda t, \\ u^- & \text{if} \quad x < \lambda t, \end{cases} \tag{1.17}$$

for some states $u^-, u^+ \in \mathbb{R}^n$, $\lambda \in \mathbb{R}$. Let any $\phi \in \mathcal{C}_c^1$ be given, and consider the linear change of variables $\tau = t,\ \ y = x - \lambda t$, so that

$$\phi_t = \phi_\tau - \lambda \phi_y, \qquad\qquad \phi_x = \phi_y \,.$$

Since ϕ has compact support, an integration by parts yields

$$\begin{aligned} 0 &= \iint \Big\{ U\,\phi_t + f(U)\,\phi_x \Big\}\ dxdt \\ &= \iint_{y<0} u^-\,\phi_\tau + \big(f(u^-) - \lambda\big)\phi_y\ dyd\tau + \iint_{y>0} u^+\,\phi_\tau + \big(f(u^+) - \lambda\big)\phi_y\ dyd\tau \\ &= \int \Big\{ \lambda\,[u^+ - u^-] - \big[f(u^+) - f(u^-)\big] \Big\} \cdot \phi(t,\,\lambda t)\ dt. \end{aligned} \tag{1.18}$$

Since (1.18) holds for every $\phi \in \mathcal{C}_c^1$, we conclude that

$$\lambda\,(u^+ - u^-) = f(u^+) - f(u^-), \tag{1.19}$$

The vector equations (1.19) are the famous *Rankine-Hugoniot conditions.* They form a set of n scalar equations relating the right and left states $u^+, u^- \in \mathbb{R}^n$ and the speed λ of the shock.

In the scalar case, (1.19) reduces to a single equation. One can thus assign u^+, u^- arbitrarily and use the equation to determine the shock speed:

$$\lambda = \frac{f(u^+) - f(u^-)}{u^+ - u^-} = \frac{1}{u^+ - u^-} \int_{u^-}^{u^+} f'(u)\ du. \tag{1.20}$$

The last expression in (1.20) shows that the shock speed coincides with the average of the characteristic speeds $f'(u)$ over the interval $[u^-, u^+]$.

Example 3. In the case of Burgers' equation $u_t + (u^2/2)_x = 0$, one finds

$$\lambda = \frac{\big[(u^+)^2/2\big] - \big[(u^-)^2/2\big]}{u^+ - u^-} = \frac{u^+ + u^-}{2}\,. \tag{1.21}$$

In the general vector case, for every couple of states $u, v \in \mathbb{R}^n$ we can define the averaged matrix

$$A(u,v) \doteq \int_0^1 A\big(\theta u + (1-\theta)v\big)\ d\theta \tag{1.22}$$

with $A = Df$ the Jacobian matrix of f, and call $\lambda_i(u,v)$ its eigenvalues. One can then write (1.19) in the equivalent form

$$\lambda\,(u^+ - u^-) = f(u^+) - f(u^-) = \int_0^1 Df\big(\theta u^+ + (1-\theta)u^-\big) \cdot (u^+ - u^-)\ d\theta = A(u^+, u^-) \cdot (u^+ - u^-). \tag{1.23}$$

In other words, the Rankine-Hugoniot equations hold iff the jump $u^+ - u^-$ is an eigenvector of the averaged matrix $A(u^+, u^-)$ and the speed λ coincides with the corresponding eigenvalue.

To extend the above Rankine-Hugoniot conditions to more general solutions, we introduce

Definition 1. We say that a function $u = u(t,x)$ has an *approximate jump discontinuity* at the point (τ, ξ) if there exists vectors $u^+ \neq u^-$ and a speed $\lambda \in \mathbb{R}$ such that, defining U as in (1.17), there holds

$$\lim_{r\to 0+} \frac{1}{r^2} \int_{-r}^{r} \int_{-r}^{r} \bigl|u(\tau + t,\ \xi + x) - U(t,x)\bigr|\, dx dt = 0. \tag{1.24}$$

Moreover, we say that u is *approximately continuous* at the point (τ, ξ) if the above relation (1.24) holds with $u^+ = u^-$ (and λ arbitrary).

Observe that the above definitions depend only on the $\mathbf{L}^1$ equivalence class of u. Indeed, the limit (1.24) is unaffected if the values of u are changed on a set $\mathcal{N} \subset \mathbb{R}^2$ of Lebesgue measure zero.

Example 4. Let $f_1, f_2 : \mathbb{R}^2 \mapsto \mathbb{R}^n$ be continuous and let $x = \gamma(t)$ be the equation of a differentiable curve. Consider a point (τ, ξ) with $\xi = \gamma(\tau)$, assuming that $f_1(\tau, x) \doteq u^- \neq u^+ \doteq f_2(\tau, \xi)$. Then the function

$$u(t,x) \doteq \begin{cases} f_1(t,x) & \text{if} \quad x < \gamma(t), \\ f_2(t,x) & \text{if} \quad x > \gamma(t). \end{cases}$$

has an approximate jump at (τ, ξ), with corresponding speed $\lambda = \dot{\gamma}(\tau)$.

We now show that the Rankine-Hugoniot equations also hold at all points of approximate jump.

Theorem 1 (Rankine-Hugoniot conditions). *Let $u = u(t,x)$ be a bounded weak solution to the system of conservation laws (1.1). Assume that u has an approximate jump at the point (τ, ξ), so that (1.24) holds with U as in (1.17). Then the equations (1.19) hold.*

Proof. For every $\nu \geq 1$, the rescaled function

$$u_\nu(t,x) \doteq u(\tau + \nu t,\ \xi + \nu x)$$

is still a weak solution of the system (1.1). As $\nu \to \infty$, by (1.24) the functions u_ν converge to U in $\mathbf{L}^1_{\rm loc}$. We conclude that the function U itself is a solution of the system (1.1), hence the Rankine-Hugoniot equations (1.19) hold.

1.5 - Entropy conditions. In the presence of discontinuities, the Rankine-Hugoniot equations (1.16) may not suffice to single out a unique solution to the Cauchy problem.

Example 5. For Burgers' equation (1.12), the Cauchy problem with initial data

$$u(0,x)=\begin{cases}1 & \text{if} \quad x\geq 0,\\ 0 & \text{if} \quad x<0,\end{cases}$$

admits infinitely many weak solutions. For every $\alpha\in[0,1]$, one can check that the piecewise constant function

$$u_\alpha(t,x)=\begin{cases}0 & \text{if} \quad x<\alpha t/2,\\ \alpha & \text{if} \quad \alpha t/2\leq x<(1+\alpha)t/2,\\ 1 & \text{if} \quad x\geq(1+\alpha)t/2,\end{cases}$$

provides a solution in the distribution sense. In particular, the Rankine-Hugoniot conditions (1.20) hold along both lines of discontinuity $\xi_1(t)=\alpha t/2,\ \ \xi_2(t)=(\alpha+1)t/2$.

By the previous example it is clear that, in order to achieve the uniqueness of solutions and their continuous dependence on the initial data, the notion of weak solution must be supplemented with further "admissibility conditions", possibly motivated by physical considerations. Some of these conditions will be presently discussed.

Admissibility Condition 1 (Vanishing viscosity). A weak solution u of (1.1) is admissible if there exists a sequence of smooth solutions u^ε to

$$u_t^\varepsilon+A(u^\varepsilon)u_x^\varepsilon=\varepsilon u_{xx}^\varepsilon \tag{1.25}$$

which converge to u in $\mathbf{L}^1_{\rm loc}$ as $\varepsilon\to 0+$.

Unfortunately, it is very difficult to provide uniform estimates on solutions to the parabolic system (1.25) and characterize the corresponding limits as $\varepsilon\to 0+$. From the above condition, however, one can deduce other conditions which can be more easily verified in practice.

A continuously differentiable function $\eta:\mathbb{R}^n\mapsto\mathbb{R}$ is called an *entropy* for the system (1.1), with *entropy flux* $q:\mathbb{R}^n\mapsto\mathbb{R}$ if

$$D\eta(u)\cdot Df(u)=Dq(u)\qquad\qquad u\in\mathbb{R}^n. \tag{1.26}$$

Observe that (1.26) implies that, if $u=u(t,x)$ is a $\mathcal{C}^1$ solution of (1.1), then

$$\big[\eta(u)\big]_t+\big[q(u)\big]_x=0. \tag{1.27}$$

Indeed,

$$D\eta(u)u_t+Dq(u)u_x=D\eta(u)\big[-Df(u)u_x\big]+Dq(u)u_x=0.$$

Hence, whenever we have a smooth solution of (1.1), not only the quantities $u_1,\ldots,u_n$ are conserved, but the additional conservation law (1.27) holds as well. On the other hand, when u is discontinuous, in general it does not provide a weak solution to (1.27), i.e. $\eta = \eta(u)$ is not a conserved quantity. This can be seen in Example 3 (Burgers' equation), taking $\eta(u) = u^3$ and $q(u) = (3/4)u^4$.

We now study how a convex entropy behaves in the presence of a small diffusion term. Assume $\eta, q \in \mathcal{C}^2$, with η convex. Multiplying both sides of (1.25) on the left by $D\eta(u^\varepsilon)$ one finds

$$\big[\eta(u^\varepsilon)\big]_t + \big[q(u^\varepsilon)\big]_x = \varepsilon D\eta(u^\varepsilon)u^\varepsilon_{xx} = \varepsilon\Big\{\big[\eta(u^\varepsilon)\big]_{xx} - D^2\eta(u^\varepsilon)\cdot\big(u^\varepsilon_x \otimes u^\varepsilon_x\big)\Big\}. \tag{1.28}$$

Observe that the last term in (1.28) satisfies

$$D^2\eta(u^\varepsilon)\big(u^\varepsilon_x \otimes u^\varepsilon_x\big) = \sum_{i,j=1}^{n} \frac{\partial^2\eta(u^\varepsilon)}{\partial u_i \partial u_j}\cdot\frac{\partial u^\varepsilon_i}{\partial x}\frac{\partial u^\varepsilon_j}{\partial x} \geq 0,$$

because η is convex, hence its second derivative at any point u^ε is a positive semidefinite quadratic form. Multiplying (1.28) by a nonnegative smooth function φ with compact support and integrating by parts, we thus have

$$\iint \big\{\eta(u^\varepsilon)\varphi_t + q(u^\varepsilon)\varphi_x\big\}\,dxdt \geq -\varepsilon\iint \eta(u^\varepsilon)\varphi_{xx}\,dxdt.$$

If $u^\varepsilon \to u$ in $\mathbf{L}^1$ as $\varepsilon \to 0$, the previous inequality yields

$$\iint \big\{\eta(u)\varphi_t + q(u)\varphi_x\big\}\,dxdt \geq 0 \tag{1.29}$$

whenever $\varphi \in \mathcal{C}^1_c$, $\varphi \geq 0$. The above can be restated by saying that $\eta(u)_t + q(u)_x \leq 0$ in distribution sense. The previous analysis leads to:

Admissibility Condition 2 (Entropy inequality). A weak solution u of (1.1) is *entropy-admissible* if

$$\big[\eta(u)\big]_t + \big[q(u)\big]_x \leq 0 \tag{1.30}$$

in the sense of distributions, for every pair (η, q), where η is a convex entropy for (1.1) and q is the corresponding entropy flux.

For the piecewise constant function U in (1.17), an application of the divergence theorem shows that $\eta(U)_t + q(U)_x \leq 0$ in distribution if and only if

$$\lambda\big[\eta(u^+) - \eta(u^-)\big] \geq q(u^+) - q(u^-). \tag{1.31}$$

More generally, let $u = u(t,x)$ be a bounded function which satisfies (1.30). Assume that u has an approximate jump at (τ, ξ), so that (1.24) holds with U as in (1.17). Then, by the rescaling argument used in the proof of Theorem 1, one can show that the inequality (1.31) must again hold.

Of course, the above admissibility condition can be useful only if some nontrivial convex entropy for the system (1.1) is known. For $n \times n$ systems, (1.26) can be regarded as a first order system of n equations for the two scalar variables η, q. When $n \geq 3$, this system is overdetermined. In general, one should thus expect to find solutions only in the case $n \leq 2$. However, there are important physical examples of larger systems which admit a nontrivial entropy function.

In the scalar case, convex entropies are easy to construct. In particular, for each $k \in \mathbb{R}$, consider the functions

$$\eta(u) = |u-k|, \qquad\qquad q(u) = \text{sgn}(u-k) \cdot \big(f(u) - f(k)\big).$$

It is easily checked that η, q are locally Lipschitz continuous and satisfy (1.26) at every $u \neq k$. Although $\eta, q \notin \mathcal{C}^1$, we can still regard η as a convex entropy for (1.1), with entropy flux q. Following Volpert [29], we say that a bounded measurable function u is an *entropic solution* of (1.1) if

$$\iint \Big\{ |u-k|\varphi_t + \text{sgn}(u-k)\big(f(u) - f(k)\big)\varphi_x \Big\}\, dxdt \geq 0 \tag{1.32}$$

for every constant $k \in \mathbb{R}$ and every $\mathcal{C}^1$ function $\varphi \geq 0$ with compact support.

According to (1.32), one can show that a shock connecting the left and right states u^-, u^+ is admissible if and only if

$$\frac{f(u^*) - f(u^-)}{u^* - u^-} \geq \frac{f(u^+) - f(u^*)}{u^+ - u^*} \tag{1.33}$$

for every $u^* = \alpha u^+ + (1-\alpha)u^-$, with $0 < \alpha < 1$. The above inequality can be interpreted as a stability condition. Indeed, let $u^* \in [u^-, u^+]$ be an intermediate state and consider a slightly perturbed solution (fig. 6a-b), where the shock (u^-, u^+) is decomposed as two separate jumps, (u^-, u^*) and (u^*, u^+), say located at $\gamma^-(t) < \gamma^+(t)$ respectively. By the the Rankine-Hugoniot conditions, the two sides of (1.33) yield precisely the speeds of these jumps. If the inequality holds, then $\dot\gamma^- \geq \dot\gamma^+$, so that the backward shock travels at least as fast as the forward one. Therefore, the two shocks will not split apart as time increases, and the perturbed solution will remain close to the original solution possessing a single shock.

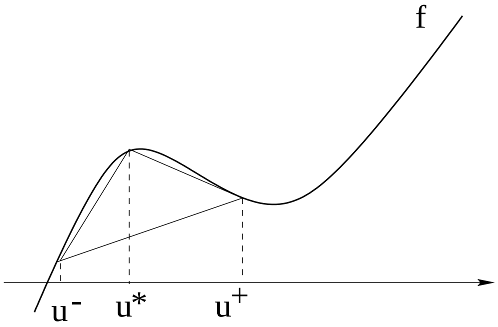

figure 7a

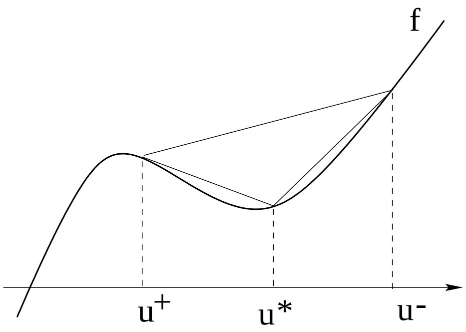

figure 7b

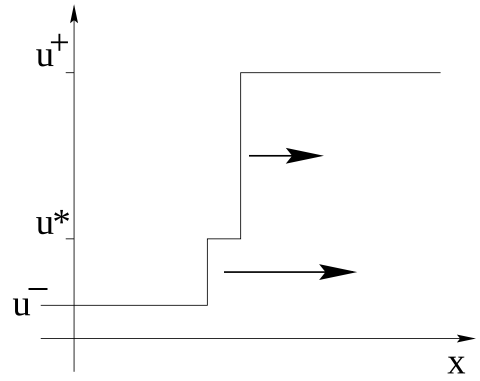

figure 6a

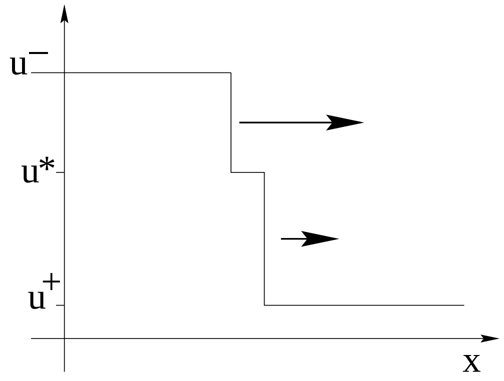

figure 6b

Observing that the Rankine-Hugoniot speed of a shock in (1.19) is given by the slope of the secant line to the graph of f through the points u^-, u^+, the condition (1.33) holds if and only if for every $\alpha \in [0,1]$ one has

$$\begin{cases} f\big(\alpha u^+ + (1-\alpha)u^-\big) \geq \alpha f(u^+) + (1-\alpha) f(u^-) & \text{if} \quad u^- < u^+, \\ f\big(\alpha u^+ + (1-\alpha)u^-\big) \leq \alpha f(u^+) + (1-\alpha) f(u^-) & \text{if} \quad u^- > u^+. \end{cases} \tag{1.34}$$

In other words, when $u^- < u^+$ the graph of f should remain above the secant line (fig.7a). When $u^- > u^+$, the graph of f should remain below the secant line (fig.7b).

A third admissibility condition, due to Lax [18], is particularly useful because it can be applied to any system of conservation laws and has a very intuitive geometrical meaning. Consider a bounded weak solution u of (1.1). By Theorem 1, the Rankine-Hugoniot conditions (1.19) hold at every point of approximate jump. According to (1.23), every shock thus travels with a speed $\lambda = \lambda_i(u^-, u^+)$ equal to an eigenvalue of the averaged matrix $A(u^-, u^+)$. In this setting, the Lax condition requires that the i-characteristics, travelling on the left and on the right of the shock with speeds $\lambda_i(u^-)$, $\lambda_i(u^+)$ respectively, both run into the shock:

Admissibility Condition 3 (Lax Condition). A bounded weak solution of the system (1.1) is *Lax admissible* if, at every point of approximate jump, the speeds corresponding to the left and right states u^-, u^+ satisfy

$$\lambda_i(u^-) \geq \lambda_i(u^-, u^+) \geq \lambda_i(u^+). \tag{1.35}$$

This situation is illustrated in fig. 8a. On the other hand, one can check that for the solutions constructed in Example 3, neither of the two shocks satisfies the above condition (fig. 8b).

1.6 - Shock and rarefaction curves. Fix a state $u_0 \in I\!R^n$ and an index $i \in \{1, \ldots, n\}$. As before, let $r_i(u)$ be the i-th eigenvector of the Jacobian matrix $A(u) = Df(u)$. The integral curve

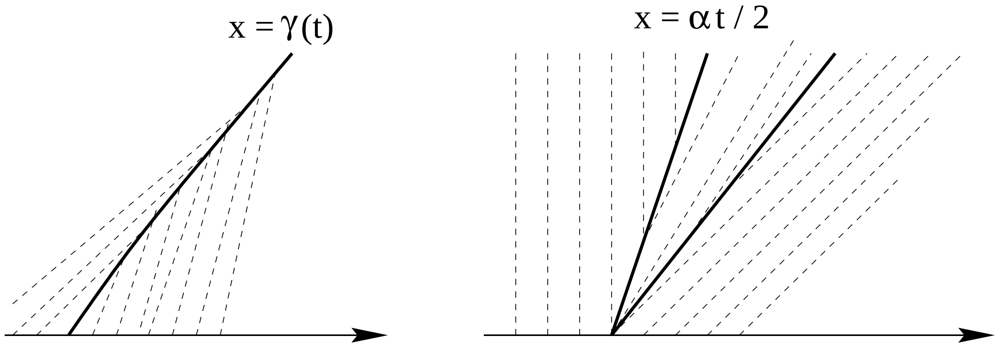

figure 8a figure 8b

of the vector field r_i through the point u_0 is called the *i-rarefaction curve* through u_0. It is obtained by solving the Cauchy problem in state space:

$$\frac{du}{d\sigma} = r_i(u), \qquad\qquad u(0) = u_0. \tag{1.36}$$

We shall denote this curve as

$$\sigma \mapsto R_i(\sigma)(u_0). \tag{1.37}$$

Of course, the parametrization depends on the choice of the eigenvectors r_i. In particular, if we impose the normalization $\big|r_i(u)\big| \equiv 1$, then the rarefaction curve (1.37) will be parametrized by arc-length.

Next, for a fixed $u_0 \in I\!R^n$ and $i \in \{1, \ldots, n\}$, we consider the curve of states u which can be connected to the right of u_0 by an i-shock, satisfying the Rankine-Hugoniot equations (1.19). According to (1.23), these equations imply that the vector $u - u_0$ is a right i-eigenvector of the averaged matrix $A(u, u_0)$. By a theorem of basic linear algebra, this holds if and only if $u - u_0$ is orthogonal to every left j-eigenvector of $A(u, u_0)$, with $j \neq i$. The Rankine-Hugoniot conditions can thus be written in the form

$$l_j(u, u_0) \cdot (u - u_0) = 0 \qquad\qquad \text{for all} \ \ j \neq i, \tag{1.38}$$

together with $\lambda = \lambda_i(u, u_0)$. We regard (1.38) as a system of $n - 1$ scalar equations in n variables (the n components of the vector u). Linearizing (1.38) at the point $u = u_0$ we obtain the linear system

$$l_j(u_0) \cdot (w - u_0) = 0 \qquad\qquad j \neq i,$$

whose solutions are all the points $w = u_0 + c r_i(u_0)$, $c \in I\!R$. By the implicit function theorem, it thus follows that the set of solutions of (1.38) is a smooth curve, tangent to the vector r_i at the point u_0. This will be called the *shock curve* through the point u_0 and denoted as

$$\sigma \mapsto S_i(\sigma)(u_0). \tag{1.39}$$

Using a suitable parametrization, the two curves R_i, S_i have a second order contact at the point u_0 (fig. 9). More precisely, the following estimates hold [18, 24].

$$\begin{cases} R_i(\sigma)(u_0) = u_0 + \sigma r_i(u_0) + \mathcal{O}(1)\cdot\sigma^2, \\ S_i(\sigma)(u_0) = u_0 + \sigma r_i(u_0) + \mathcal{O}(1)\cdot\sigma^2, \end{cases} \tag{1.40}$$

$$\big|R_i(\sigma)(u_0) - S_i(\sigma)(u_0)\big| = \mathcal{O}(1)\cdot\sigma^3, \tag{1.41}$$

$$\lambda_i\big(S_i(\sigma)(u_0),\quad u_0\big) = \lambda_i(u_0) + \frac{\sigma}{2}\big(D\lambda_i(u_0)\big)\cdot r_i(u_0) + \mathcal{O}(1)\cdot\sigma^2. \tag{1.42}$$

Here and throughout the following, the Landau symbol $\mathcal{O}(1)$ denotes a quantity whose absolute value satisfies a uniform bound, depending only on the system (1.1).

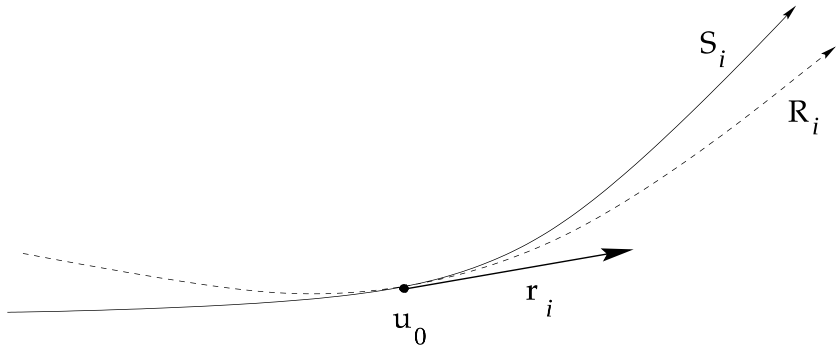

figure 9

1.7 - The Riemann problem. The basic building block toward the solution of the general Cauchy problem for (1.1) is the the solution of the following initial value problem:

$$u_t + f(u)_x = 0, \qquad\qquad u(0,x) = \bar u(x) \doteq \begin{cases} u^- & \text{if} \quad x < 0, \\ u^+ & \text{if} \quad x > 0. \end{cases} \tag{1.43}$$

The initial data have here a very simple form, being constant for $x < 0$ and for $x > 0$, with a single jump at the origin.

Before describing the general solution of (1.43), a key assumption will be introduced. Recall that $\lambda_i(u)$, $r_i(u)$ denote the i-th eigenvalue and the i-th right eigenvector of the matrix $A(u) = Df(u)$. Following [18], the i-th characteristic field is called *genuinely nonlinear* if $D\lambda_i(u)\cdot r_i(u) \neq 0$ for all u. On the other hand, if $D\lambda_i(u)\cdot r_i(u) = 0$ for all u, we say that the i-th field is *linearly degenerate*. In the genuinely nonlinear case, we can choose the orientation of the eigenvectors r_i so that

$$D\lambda_i(u)\cdot r_i(u) > 0. \tag{1.44}$$

Therefore, if the i-th characteristic field is genuinely nonlinear, then the characteristic speed λ_i is monotonically increasing along the i-rarefaction curves (1.37). On the other hand, if the i-th field is linearly degenerate, then λ_i is constant along the curves R_i. Throughout the following, a solution of the Riemann problem will be constructed under the following assumptions:

(♣) The system (1.1) is strictly hyperbolic with smooth coefficients. For each $i \in \{1, \ldots, n\}$, the i-th characteristic field is either genuinely nonlinear or linearly degenerate.

We shall first study three special cases:

1 - Centered Rarefaction Waves. Let the i-th field be genuinely nonlinear, and assume that u^+ lies on the positive i-rarefaction curve through u^-, i.e. $u^+ = R_i(\sigma)(u^-)$ for some $\sigma > 0$. For each $s \in [0, \sigma]$, define

$$\lambda_i(s) = \lambda_i\big(R_i(s)(u^-)\big).$$

By genuine nonlinearity, the map $s \mapsto \lambda_i(s)$ is strictly increasing. For $t \geq 0$, the function

$$u(t,x) = \begin{cases} u^- & \text{if} \quad x/t < \lambda_i(u^-), \\ R_i(s)(u^-) & \text{if} \quad x/t = \lambda_i(s) \in \big[\lambda_i(u^-),\ \lambda_i(u^+)\big], \\ u^+ & \text{if} \quad x > t\lambda_i(u^+), \end{cases} \tag{1.45}$$

is then a piecewise smooth weak solution of the Riemann problem (1.43). Indeed,

$$\lim_{t \to 0+} \big\| u(t, \cdot) - \bar{u} \big\|_{\mathbf{L}^1} = 0.$$

Moreover, the equation (1.6) is trivially satisfied in the sectors where $x < t\lambda_i(u^-)$ or $x > t\lambda_i(u^+)$, since here $u_t = u_x = 0$. Next, assume $x = t\lambda_i(s)$ for some $s \in]0, \sigma[$. Since u is constant along each ray through the origin, of the form $x/t =$ constant, we clearly have

$$u_t(t,x) + \frac{x}{t}\, u_x(t,x) = 0. \tag{1.46}$$

We now observe that the definition (1.45) implies $x/t = \lambda_i\big(u(t,x)\big)$. Moreover, u_x is parallel to $r_i(u)$, hence it is an eigenvector of the matrix $A(u)$ with eigenvalue $\lambda_i(u)$. From (1.46) it thus follows (1.6).

Notice that the assumption $\sigma > 0$ is essential for the validity of this construction. In the opposite case $\sigma < 0$, the definition (1.45) would yield a triple-valued function in the region where $x/t \in \big[\lambda_i(u^+),\ \lambda_i(u^-)\big]$.

2 - Shocks. Assume again that the i-th family is genuinely nonlinear and that the state u^+ is connected to the right of u^- by an i-shock, i.e. $u^+ = S_i(\sigma)(u^-)$. Then, calling $\lambda \doteq \lambda_i(u^+, u^-)$ the Rankine-Hugoniot speed of the shock, the function

$$u(t,x) = \begin{cases} u^- & \text{if} \quad x < \lambda t, \\ u^+ & \text{if} \quad x > \lambda t, \end{cases} \tag{1.47}$$

provides a piecewise constant solution to the Riemann problem. Observe that, if $\sigma < 0$, than this solution is entropy admissible in the sense of Lax. Indeed, since the speed is monotonically increasing along the shock curve, recalling (1.42) we have

$$\lambda_i(u^+) < \lambda_i(u^-, u^+) < \lambda_i(u^-). \tag{1.48}$$

In the case $\sigma > 0$, however, one has $\lambda_i(u^-) < \lambda_i(u^+)$ and the admissibility condition (1.35) is violated.

3 - Contact discontinuities. Assume that the i-th field is linearly degenerate and that the state u^+ lies on the i-th rarefaction curve through u^-, i.e. $u^+ = R_i(\sigma)(u^-)$ for some σ. By assumption, the i-th characteristic speed λ_i is constant along this curve. Choosing $\lambda = \lambda(u^-)$, the piecewise constant function (1.47) then provides a solution to the Riemann problem (1.43). Indeed, the Rankine-Hugoniot conditions hold at the point of jump:

$$\begin{aligned} f(u^+) - f(u^-) &= \int_0^\sigma Df\big(R_i(s)(u^-)\big)\, r_i\big(R_i(s)(u^-)\big)\ ds \\ &= \lambda_i(u^-) \cdot \big[R_i(\sigma)(u^-) - u^-\big]. \end{aligned} \tag{1.49}$$

In this case, the Lax entropy conditions hold regardless of the sign of σ. Indeed,

$$\lambda_i(u^+) = \lambda_i(u^-, u^+) = \lambda_i(u^-). \tag{1.50}$$

Observe that, according to (1.49), for linearly degenerate fields the shock and rarefaction curves actually coincide, i.e. $S_i(\sigma)(u_0) = R_i(\sigma)(u_0)$ for all σ.

The above results can be summarized as follows. For a fixed left state u^- and $i \in \{1, \ldots, n\}$ define the mixed curve

$$\Psi_i(\sigma)(u^-) = \begin{cases} R_i(\sigma)(u^-) & \text{if} \quad \sigma \geq 0, \\ S_i(\sigma)(u^-) & \text{if} \quad \sigma < 0. \end{cases} \tag{1.51}$$

In the special case where $u^+ = \Psi_i(\sigma)(u^-)$ for some σ, the Riemann problem can then be solved by an elementary wave: a rarefaction, a shock or a contact discontinuity.

Relying on the previous analysis, the solution of the general Riemann problem (1.43) can now be obtained by finding intermediate states $\omega_0 = u^-$, $\omega_1, \ldots,$ $\omega_n = u^+$ such that each pair of adiacent states ω_{i-1}, ω_i can be connected by an elementary wave, i. e.

$$\omega_i = \Psi_i(\sigma_i)(\omega_{i-1}) \qquad\qquad i = 1, \ldots, n. \tag{1.52}$$

This can be done whenever u^+ is sufficiently close to u^-. Indeed, for $|u^+ - u^-|$ small, the implicit function theorem provides the existence of unique wave strengths $\sigma_1, \ldots \sigma_n$ such that

$$u^+ = \Psi_n(\sigma_n) \circ \cdots \circ \Psi_1(\sigma_1)(u^-). \tag{1.53}$$

In turn, these determine the intermediate states ω_i in (1.52). The solution to (1.43) is now obtained by piecing together the solutions of the n Riemann problems

$$u_t + f(u)_x = 0, \qquad u(0,x) = \begin{cases} \omega_{i-1} & \text{if} \quad x < 0, \\ \omega_i & \text{if} \quad x > 0 \end{cases} \tag{1.54}$$

on different sectors of the t-x plane. By construction, each of these problems has an entropy-admissible solution consisting of a simple wave of the i-th characteristic family. More precisely:

CASE 1: The i-th characteristic field is genuinely nonlinear and $\sigma_i > 0$. Then the solution of (1.54) consists of a centered rarefaction wave. The i-th characteristic speeds range over the interval $[\lambda_i^-, \lambda_i^+]$, defined as

$$\lambda_i^- \doteq \lambda_i(\omega_{i-1}), \qquad \lambda_i^+ \doteq \lambda_i(\omega_i). \tag{1.55}$$

CASE 2: Either the i-th characteristic field is genuinely nonlinear and $\sigma_i \leq 0$, or else the i-th characteristic field is linearly degenerate (with σ_i arbitrary). Then the solution of (1.54) consists of an admissible shock or of a contact discontinuity, travelling with Rankine-Hugoniot speed

$$\lambda_i^- \doteq \lambda_i^+ \doteq \lambda_i(\omega_{i-1}, \omega_i). \tag{1.56}$$

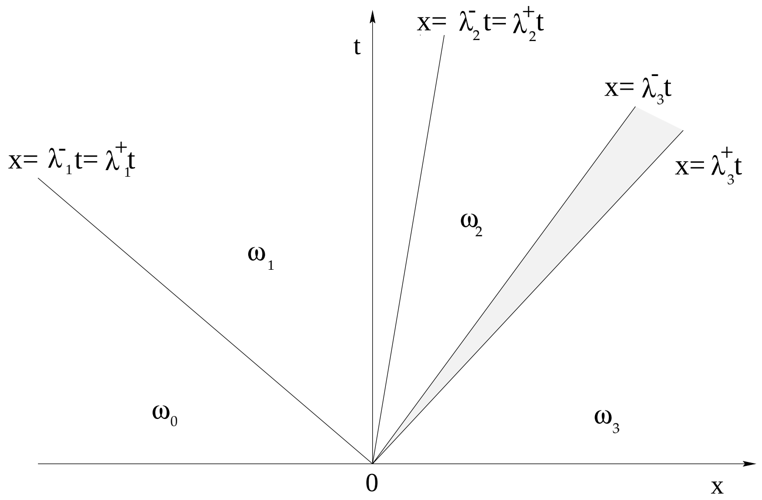

figure 10

The solution to the original problem (1.43) can now be constructed (fig. 10) by piecing together the solutions of the n Riemann problems (1.54), $i = 1, \ldots, n$. Indeed, for $\sigma_1, \ldots, \sigma_n$ sufficiently small, the speeds λ_i^-, λ_i^+ introduced at (1.55) or (1.56) remain close to the corresponding eigenvalues $\lambda_i(u^-)$ of the matrix $A(u^-)$. By strict hyperbolicity and continuity, we can thus assume that the n intervals $[\lambda_i^-, \lambda_i^+]$ are disjoint, i.e.

$$\lambda_1^- \leq \lambda_1^+ \; < \; \lambda_2^- \leq \lambda_2^+ \; < \cdots < \; \lambda_n^- \leq \lambda_n^+.$$

Therefore, a piecewise smooth solution $u : [0,\infty) \times I\!R \mapsto I\!R^n$ is well defined by the assignment:

$$u(t,x) = \begin{cases} u^- = \omega_0 & \text{if} \quad \dfrac{x}{t} \in \big]-\infty,\ \lambda_1^-\big[, \\ R_i(s)(\omega_{i-1}) & \text{if} \quad \dfrac{x}{t} = \lambda_i\big(R_i(s)(\omega_{i-1})\big) \in \big[\lambda_i^-,\ \lambda_i^+\big[, \\ \omega_i & \text{if} \quad \dfrac{x}{t} \in \big[\lambda_i^+,\ \lambda_{i+1}^-\big[\\ u^+ = \omega_n & \text{if} \quad \dfrac{x}{t} \in \big[\lambda_n^+,\ \infty\big[\,. \end{cases} \tag{1.57}$$

Observe that this solution is self-similar, having the form $u(t,x) = \psi(x/t)$, with $\psi : I\!R \mapsto I\!R^n$ generally discontinuous.

Example 6. The 2×2 system of conservation laws

$$[u_1]_t + \left[\frac{u_1}{1+u_1+u_2}\right]_x = 0, \qquad [u_2]_t + \left[\frac{u_2}{1+u_1+u_2}\right]_x = 0, \qquad u_1, u_2 > 0, \tag{1.58}$$

is motivated by the study of two-component chromatography. Writing (1.58) in the quasilinear form (1.6), the eigenvalues and eigenvectors of the corresponding 2×2 matrix $A(u)$ are found to be

$$\lambda_1(u) = \frac{1}{(1+u_1+u_2)^2}, \qquad \lambda_2(u) = \frac{1}{1+u_1+u_2},$$

$$r_1(u) = \frac{1}{\sqrt{u_1^2+u_2^2}} \cdot \begin{pmatrix} -u_1 \\ -u_2 \end{pmatrix}, \qquad r_2(u) = \frac{1}{\sqrt{2}} \cdot \begin{pmatrix} 1 \\ -1 \end{pmatrix}.$$

The first characteristic field is genuinely nonlinear, the second is linearly degenerate. In this example, the two shock and rarefaction curves S_i, R_i always coincide, for $i = 1, 2$. Their computation is easy, because they are straight lines (fig. 11):

$$R_1(\sigma)(u) = u + \sigma r_1(u), \qquad R_2(\sigma)(u) = u + \sigma r_2(u). \tag{1.59}$$

Observe that the integral curves of the vector field r_1 are precisely the rays through the origin, while the integral curves of r_2 are the lines with slope -1. Now let two states $u^- = (u_1^-, u_2^-)$, $u^+ = (u_1^+, u_2^+)$ be given. To solve the Riemann problem (1.43), we first compute an intermediate state u^* such that $u^* = R_1(\sigma_1)(u^-)$, $\quad u^+ = R_2(\sigma_2)(u^*)$ for some σ_1, σ_2. By (1.59), the components of u^* satisfy

$$u_1^* + u_2^* = u_1^+ + u_2^+, \qquad u_1^* u_2^- = u_1^- u_2^*.$$

The solution of the Riemann problem thus takes two different forms, depending on the sign of $\sigma_1 = \sqrt{(u_1^-)^2 + (u_2^-)^2} - \sqrt{(u_1^*)^2 + (u_2^*)^2}$.

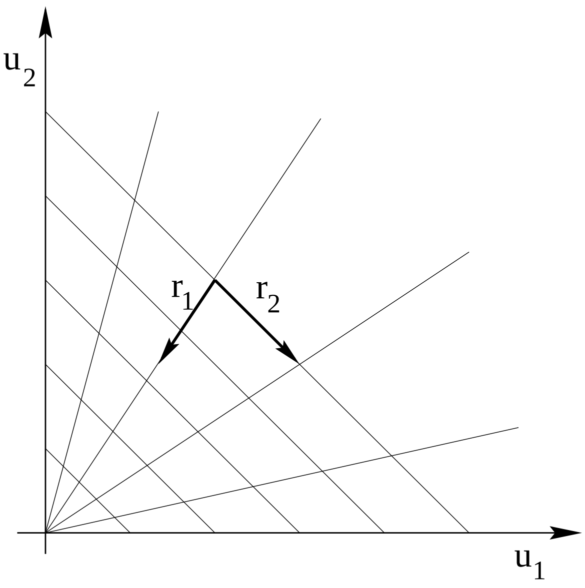

figure 11

CASE 1: $\sigma_1 > 0$. Then the solution consists of a centered rarefaction wave of the first family and of a contact discontinuity of the second family:

$$u(t,x) = \begin{cases} u^- & \text{if} \quad x/t < \lambda_1(u^-), \\ su^* + (1-s)u^- & \text{if} \quad x/t = \lambda_1\big(su^* + (1-s)u^-\big), \qquad s \in [0,1], \\ u^* & \text{if} \quad \lambda_1(u^*) < x/t < \lambda_2(u^+), \\ u^+ & \text{if} \quad x/t \geq \lambda_2(u^+). \end{cases} \tag{1.60}$$

CASE 2: $\sigma_1 \leq 0$. Then the solution contains a compressive shock of the first family (which vanishes if $\sigma_1 = 0$) and a contact discontinuity of the second family:

$$u(t,x) = \begin{cases} u^- & \text{if} \quad x/t < \lambda_1(u^-, u^*), \\ u^* & \text{if} \quad \lambda_1(u^-, u^*) \leq x/t < \lambda_2(u^+), \\ u^+ & \text{if} \quad x/t \geq \lambda_2(u^+). \end{cases} \tag{1.61}$$

Observe that $\lambda_2(u^*) = \lambda_2(u^+) = (1 + u_1^+ + u_2^+)^{-1}$, because the second characteristic field is linearly degenerate. In this special case, since the integral curves of r_1 are straight lines, the shock speed in (1.61) can be computed as

$$\begin{aligned} \lambda_1(u^-, u^*) &= \int_0^1 \lambda_1\big(su^* + (1-s)u^-\big)\, ds \\ &= \int_0^1 \big[1 + s(u_1^* + u_2^*) + (1-s)(u_1^- + u_2^-)\big]^{-2}\, ds \\ &= \frac{1}{(1 + u_1^* + u_2^*)(1 + u_1^- + u_2^-)}. \end{aligned}$$

Example 7. A model for isentropic gas dynamics (in Lagrangian coordinates) is provided by the following 2×2 hyperbolic system:

$$v_t - u_x = 0, \qquad\qquad u_t + p(v)_x = 0. \tag{1.62}$$

Here $v > 0$ is the specific volume, i.e. $v = \rho^{-1}$ where ρ is the density, and u is the velocity. The function $p = p(v)$ gives the pressure in terms of the specific volume. It is thus natural to assume

$$p > 0, \qquad p' < 0, \qquad p'' > 0. \tag{1.63}$$

A typical choice, valid for most gases, is

$$p(v) = \frac{k}{v^\gamma}, \qquad\qquad 1 < \gamma < 3.$$

Here γ is called the *adiabatic gas constant.* On the region where $v > 0$, the system is strictly hyperbolic. Indeed, the Jacobian matrix

$$A \doteq Df = \begin{pmatrix} 0 & -1 \\ p'(v) & 0 \end{pmatrix}$$

has real and distinct eigenvalues

$$\lambda_1 = -\sqrt{-p'(v)}, \qquad\qquad \lambda_2 = \sqrt{-p'(v)}.$$

Introducing the vectors

$$U \doteq (v,\ u) \qquad\qquad F(U) \doteq \big(-u,\ p(v)\big),$$

the system (1.62) can be written in the standard form

$$U_t + \big[F(U)\big]_x = 0. \tag{1.64}$$

If the assumptions (1.63) hold, then the system (1.64) is strictly hyperbolic. Indeed, the Jacobian matrix

$$A(U) \doteq DF(U) = \begin{pmatrix} 0 & -1 \\ p'(v) & 0 \end{pmatrix}$$

has the two real distinct eigenvalues

$$\lambda_1 = -\sqrt{-p'(v)} < 0 < \sqrt{-p'(v)} = \lambda_2, \tag{1.65}$$

with corresponding (unnormalized) eigenvectors

$$r_1 = \big(1,\ \sqrt{-p'(v)}\big), \qquad\qquad r_2 = \big(-1,\ \sqrt{-p'(v)}\big).$$

We now study the Riemann problem for the system (1.64), with initial data

$$U(0,x) = \begin{cases} U^- = (v^-, u^-) & \text{if} \quad x < 0, \\ U^+ = (v^+, u^+) & \text{if} \quad x > 0, \end{cases} \tag{1.67}$$

assuming, that $v^-, v^+ > 0$.

By (1.66), the 1-rarefaction curve through U^- is obtained by solving the Cauchy problem

$$\frac{du}{dv} = \sqrt{-p'(v)}, \qquad\qquad u(v^-) = u^-.$$

This yields the curve

$$R_1 = \left\{(v,u); \quad u - u^- = \int_{v^-}^{v} \sqrt{-p'(y)}\ dy\right\}. \tag{1.68}$$

Similarly, the 2-rarefaction curve through the point U^- is

$$R_2 = \left\{(v,u); \quad u - u^- = -\int_{v^-}^{v} \sqrt{-p'(y)}\ dy\right\}. \tag{1.69}$$

Next, the shock curves S_1, S_2 through U^- are derived from the Rankine-Hugoniot conditions

$$\lambda(v - v^-) = -(u - u^-), \qquad\qquad \lambda(u - u^-) = p(v) - p(v^-). \tag{1.70}$$

Using the first equation in (1.70) to eliminate λ, these shock curves are computed as

$$S_1 = \left\{(v,u); \qquad -(u-u^-)^2 = (v-v^-)\big(p(v) - p(v^-)\big), \quad \lambda \doteq -\frac{u-u^-}{v-v^-} < 0\right\}, \tag{1.71}$$

$$S_2 = \left\{(v,u); \qquad -(u-u^-)^2 = (v-v^-)\big(p(v) - p(v^-)\big), \quad \lambda \doteq -\frac{u-u^-}{v-v^-} > 0\right\}. \tag{1.72}$$

Recalling (1.65)-(1.66) and the assumptions (1.63), we now compute the directional derivatives

$$(D\lambda_1)r_i = (D\lambda_2)r_2 = \frac{p''(v)}{2\sqrt{-p'(v)}} > 0. \tag{1.73}$$

By (1.73) it is clear that the Riemann problem (1.64), (1.67) admits a solution in the form of a centered rarefaction wave in the two cases $U^+ \in R_1$, $v^+ > v^-$, or else $U^+ \in R_2$, $v^+ < v^-$. On the other hand, a shock connecting U^- with U^+ will be admissible provided that either $U^+ \in S_1$ and $v^+ < v^-$, or else $U^+ \in S_2$ and $v^+ > v^-$.

Taking the above admissibility conditions into account, we thus obtain four lines originating from the point $U^- = (v^-, u^-)$, i.e. the two rarefaction curves

$$\sigma \mapsto R_1(\sigma),\ R_2(\sigma) \qquad\qquad \sigma \geq 0,$$

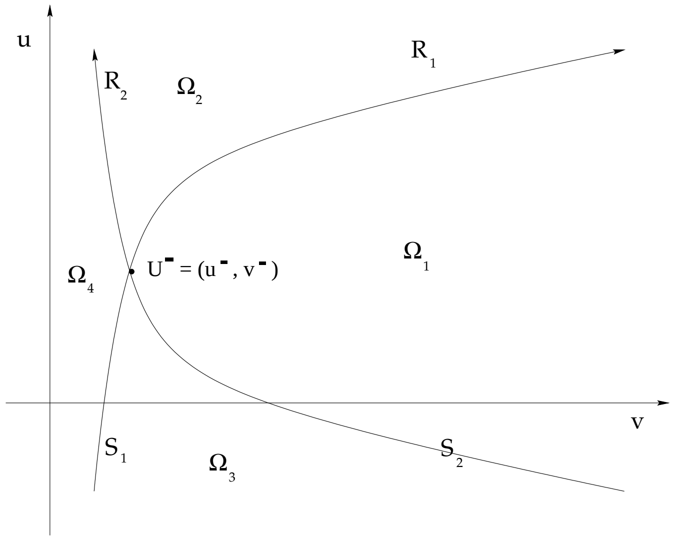

figure 12

and the two shock curves

$$\sigma \mapsto S_1(\sigma),\ S_2(\sigma) \qquad\qquad \sigma \leq 0.$$

In turn, these curves divide a neighborhood of U^- into four regions (fig 12):

$$\Omega_1,\ \text{bordering on}\ \ R_1, S_2, \qquad\qquad \Omega_2,\ \ \text{bordering on}\ \ R_1, R_2,$$
$$\Omega_3,\ \text{bordering on}\ \ S_1, S_2, \qquad\qquad \Omega_4,\ \ \text{bordering on}\ \ S_1, R_2.$$

For U^+ sufficiently close to U^-, the structure of the general solution to the Riemann problem is now determined by the location of the state U^+, with respect to the curves R_i, S_i (fig 13).

CASE 1: $U^+ \in \Omega_1$. The solution consists of a 1-rarefaction wave and a 2-shock.

CASE 2: $U^+ \in \Omega_2$. The solution consists of two centered rarefaction waves.

CASE 3: $U^+ \in \Omega_3$. The solution consists of two shocks.

CASE 4: $U^+ \in \Omega_4$. The solution consists of a 1-shock and a 2-rarefaction wave.

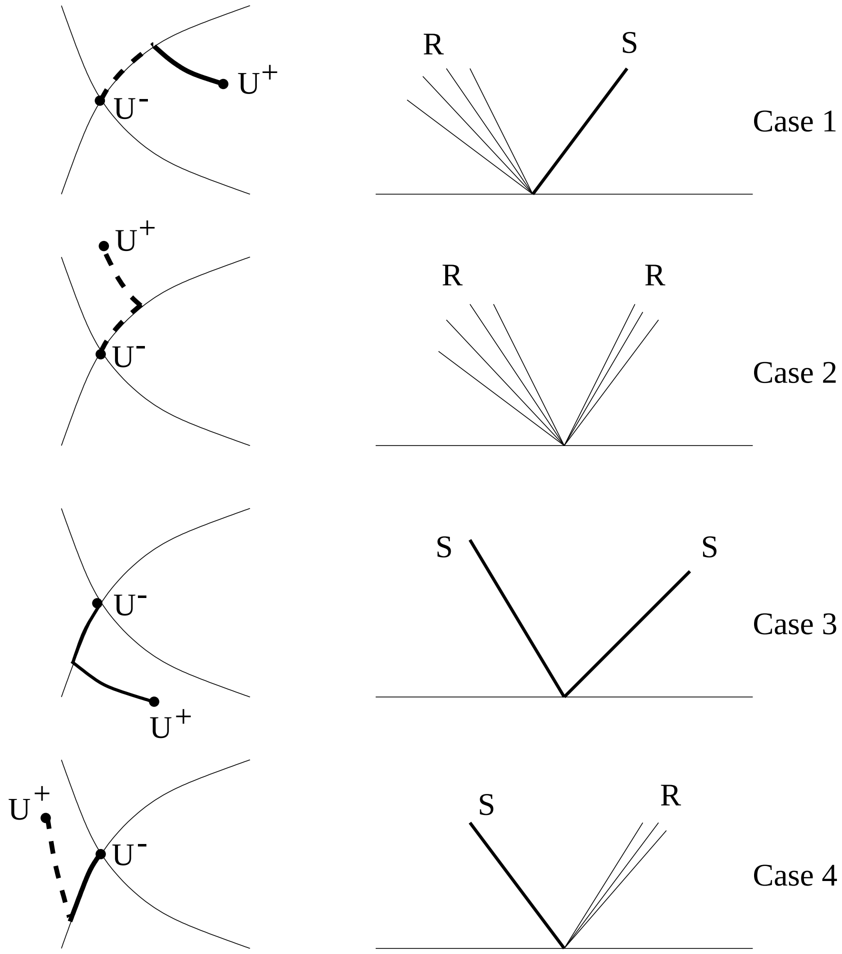

figure 13

2 - Wave-front tracking approximations.

The main goal of this chapter is to prove the global existence of a weak, entropy admissible solution to the Cauchy problem

$$u_t + f(u)_x = 0, \tag{2.1}$$

$$u(0,x) = \bar{u}(x), \tag{2.2}$$

for every integrable initial data $\bar{u}$ with sufficiently small total variation.

Theorem 2. *Let the system (2.1) be strictly hyperbolic and assume that each characteristic field is either linearly degenerate or genuinely nonlinear. Then there exists a constant $\delta > 0$ such that, for every initial condition $\bar{u} \in \mathbf{L}^1(I\!R;\ I\!R^n)$ with*

$$Tot.Var.(\bar{u}) \leq \delta, \tag{2.3}$$

the Cauchy problem (2.1)-(2.2) has an entropy admissible weak solution $u = u(t, x)$ defined for all $t \geq 0$.

Theorem 2 was first proved in the fundamental paper of Glimm [15], constructing approximate solutions by means of a random restarting procedure.
Here we shall describe an alternative method for constructing approximate solutions, based on wave-front tracking. Roughly speaking, a front tracking ε-approximate solution (fig. 14) is a piecewise constant function $u = u(t, x)$ whose jumps are located along finitely many segments $x = x_\alpha(t)$ in the t-x plane. At each time $t > 0$, these jumps should approximately satisfy the Rankine-Hugoniot conditions

$$\sum_\alpha \Big| \dot{x}_\alpha \big[u(t, x_\alpha+) - u(t, x_\alpha-) \big] - \big[f(u(t, x_\alpha+)) - f(u(t, x_\alpha-)) \big] \Big| = \mathcal{O}(1) \cdot \varepsilon.$$

If η is a convex entropy with flux q, recalling (1.27), at each time t one should also have

$$\sum_\alpha \Big\{ \big[q(u(t, x_\alpha+)) - q(u(t, x_\alpha-)) \big] - \dot{x}_\alpha \big[\eta(u(t, x_\alpha+)) - \eta(u(t, x_\alpha-)) \big] \Big\} \leq \mathcal{O}(1) \cdot \varepsilon.$$

In practice, since we want to use these approximations for a detailed analysis of solutions, it is convenient to require a number of additional properties, described below.

Definition 2. *Given $\varepsilon > 0$, we say that $u : [0, \infty[\mapsto \mathbf{L}^1(I\!R;\ I\!R^n)$ is an ε-approximate front tracking solution of (2.1) if the following holds:*

1. *As a function of two variables, $u = u(t, x)$ is piecewise constant, with discontinuities occurring along finitely many lines in the t-x plane. Only finitely many wave-front interactions occur, each involving exactly two incoming fronts. Jumps can be of three types: shocks (or contact discontinuities), rarefactions and non-physical waves, denoted as $\mathcal{J} = \mathcal{S} \cup \mathcal{R} \cup \mathcal{NP}$.*

2. *Along each shock (or contact discontinuity) $x = x_\alpha(t)$, $\alpha \in \mathcal{S}$, the values $u^- \doteq u(t, x_\alpha-)$ and $u^+ \doteq u(t, x_\alpha+)$ are related by*

$$u^+ = S_{k_\alpha}(\sigma_\alpha)(u^-), \tag{2.4}$$

for some $k_\alpha \in \{1, \ldots, n\}$ and some wave size σ_α. If the k_α-th family is genuinely nonlinear, then the entropy admissibility condition $\sigma_\alpha < 0$ also holds. Moreover, the speed of the shock front satisfies

$$\big| \dot{x}_\alpha - \lambda_{k_\alpha}(u^+, u^-) \big| \leq \varepsilon. \tag{2.5}$$

3. *Along each rarefaction front $x = x_\alpha(t)$, $\alpha \in \mathcal{R}$, one has*

$$u^+ = R_{k_\alpha}(\sigma_\alpha)(u^-), \qquad \sigma_\alpha \in]0, \varepsilon] \tag{2.6}$$

for some genuinely nonlinear family k_α. Moreover,

$$\left|\dot x_\alpha(t) - \lambda_{k_\alpha}(u^+)\right| \leq \varepsilon. \tag{2.7}$$

4. *All non-physical fronts $x = x_\alpha(t)$, $\alpha \in \mathcal{NP}$ have the same speed:*

$$\dot x_\alpha(t) \equiv \hat\lambda, \tag{2.8}$$

where $\hat\lambda$ is a fixed constant strictly greater than all characteristic speeds. The total strength of all non-physical fronts in $u(t,\cdot)$ remains uniformly small, namely

$$\sum_{\alpha\in\mathcal{NP}} \left|u(t,x_\alpha+) - u(t,x_\alpha-)\right| \leq \varepsilon \qquad\qquad \text{for all } t \geq 0. \tag{2.9}$$

If, in addition, the initial value of u satisfies

$$\left\|u(0,\cdot) - \bar u\right\|_{\mathbf{L}^1} < \varepsilon, \tag{2.10}$$

we say that u is an ε-approximate solution to the Cauchy problem (2.1)-(2.2).

Toward a proof of Theorem 2, we shall first establish the existence of front tracking approximations.

Theorem 3. *For every $\varepsilon > 0$ and every initial data $\bar u$ with sufficiently small total variation, the Cauchy problem (2.1)-(2.2) admits an ε-approximate front tracking solution, defined for all $t \geq 0$.*

In a second step, we will show that a suitable sequence of front tracking approximations converges to a limit, providing an entropy weak solution to the Cauchy problem.

We now describe an algorithm which generates these front tracking approximations. The basic ideas were introduced in the papers of Dafermos [12] for scalar equations and Di Perna [13] for 2×2 systems, then extended in [1, 3, 21] to general $n\times n$ systems. The construction (fig. 14) starts at time $t=0$ by taking a piecewise constant approximation $u(0,\cdot)$ of $\bar u$ satisfying (2.10), with Tot.Var.$\big\{u(0,\cdot)\big\} \leq$ Tot.Var.$\{\bar u\}$. Let $x_1 < \cdots < x_N$ be the points where $u(0,\cdot)$ is discontinuous. For each $\alpha = 1,\ldots,N$, the Riemann problem generated by the jump $\big(u(0,x_\alpha-),\ u(0,x_\alpha+)\big)$ is approximately solved on a forward neighborhood of $(0,x_\alpha)$ in the t-x plane by a function of the form $u(t,x) = \varphi\big((x-x_\alpha)/t\big)$, with $\varphi : I\!R \mapsto I\!R^n$ piecewise constant. More precisely, if the exact solution of the Riemann problem contains only shocks and contact discontinuities, then we let u coincide with the exact solution, which is already piecewise constant. On the other hand,

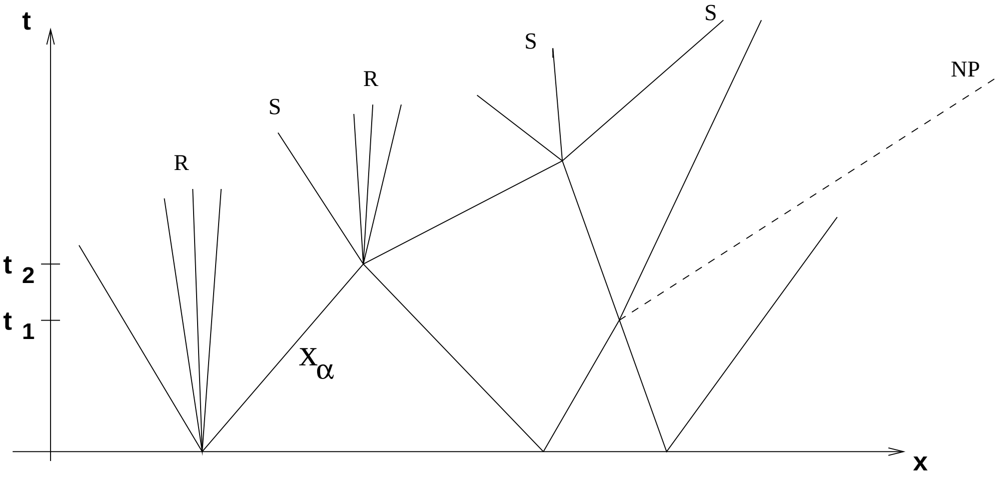

figure 14

if centered rarefaction waves are present, they are approximated by a *centered rarefaction fan*, containing several small jumps travelling with a speed close to the characteristic speed.

The approximate solution u can then be prolonged until a time t_1 is reached, when the first set of interactions between two or more wave-fronts takes place. Since $u(t_1, \cdot)$ is still a piecewise constant function, the corresponding Riemann problems can again be approximately solved within the class of piecewise constant functions. The solution u is then continued up to a time t_2 where the second set of wave interactions takes place, etc...

For general $n \times n$ systems, the main source of technical difficulty stems from the fact that the number of wave-fronts may approach infinity in finite time, in which case the construction would break down. To see this, observe that at a generic interaction point there will be two incoming fronts, while the number of outgoing fronts is n (if all waves generated by the Riemann problem are shocks or contact discontinuities), or even larger (if rarefaction waves are present). In turn, these outgoing wave-fronts may quickly interact with several other fronts, generating more and more lines of discontinuity (see fig. 15a).

We thus need to modify the algorithm, to ensure that the number of fronts will not become infinite within finite time. Following [1, 3], we will use two different procedures for solving a Riemann problem within the class of piecewise constant functions: An Accurate Riemann Solver (fig. 16a), which introduces several new wave-fronts, and a Simplified Riemann Solver (fig. 16b), which involves a minimum number of outgoing fronts. In this second case, all new waves are lumped together in a single *non-physical* front, travelling with a fixed speed $\hat{\lambda}$ strictly larger than all characteristic speeds. The main feature of this algorithm is illustrated in fig. 15a-b. If all Riemann problems were solved accurately, the number of wave-fronts could approach infinity within a finite time τ (fig. 15a). However, since the total variation remains small, the new fronts generated by

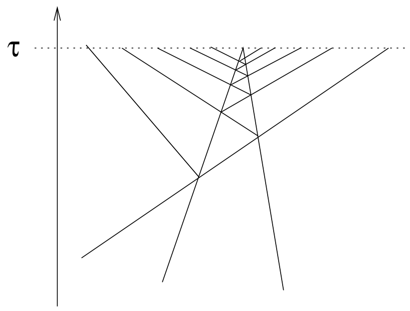

figure 15a

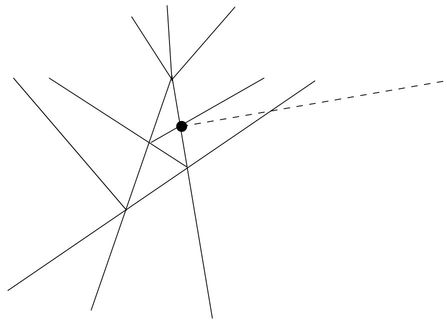

figure 15b

accurate Riemann solver

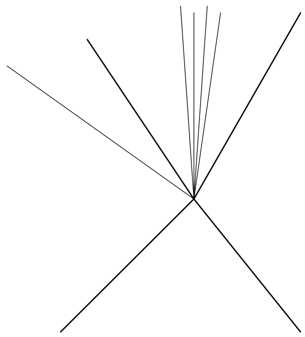

figure 16a

simplified Riemann solver

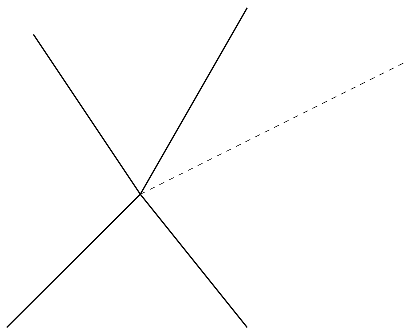

figure 16b

further interactions are very small. When their size becomes smaller than a threshold parameter $\rho > 0$, a Simplified Riemann Solver is used, which generates one single new (non-physical) front, with very small amplitude. The total number of fronts thus remains bounded for all times (fig. 15b).

Given a general Riemann problem at a point $(\bar{t}, \bar{x})$,

$$v_t + f(v)_x = 0, \qquad\qquad v(\bar{t}, x) = \begin{cases} u^- & \text{if } \ x < \bar{x}, \\ u^+ & \text{if } \ x > \bar{x}, \end{cases} \tag{2.11}$$

we now describe two procedures, which yield approximate solutions within the class of piecewise constant functions. As in the previous chapter, for a given state $u \in I\!R^n$, we denote respectively by

$$\sigma \mapsto R_i(\sigma)(u), \qquad \sigma \mapsto S_i(\sigma)(u) \qquad\qquad (i = 1, \ldots, n) \tag{2.12}$$

the i-rarefaction and i-shock curve through the state u. Moreover, we set

$$\Psi_i(\sigma)(u) \doteq \begin{cases} R_i(\sigma)(u) & \text{if} \qquad \sigma \geq 0, \\ S_i(\sigma)(u) & \text{if} \qquad \sigma < 0. \end{cases} \tag{2.13}$$

Accurate Riemann Solver.

Given u^-, u^+, we first determine the states $\omega_0, \omega_1, \ldots, \omega_n$ and parameter values $\sigma_1, \ldots, \sigma_n$ such that

$$\omega_0 = u^-, \quad \omega_n = u^+, \qquad \omega_i = \Psi_i(\sigma_i)(\omega_{i-1}) \qquad i = 1, \ldots, n. \tag{2.14}$$

Of course, $\omega_0, \ldots, \omega_n$ are the constant states present in the exact solution of the Riemann problem. If all jumps (ω_{i-1}, ω_i) were shocks or contact discontinuities, then the Riemann problem would have a piecewise constant solution with $\leq n$ lines of discontinuity. In the general case, the exact solution of (2.11) is not piecewise constant, because of the presence of rarefaction waves. These will be approximated by piecewise constant rarefaction fans, inserting additional states $\omega_{i,j}$ as follows.

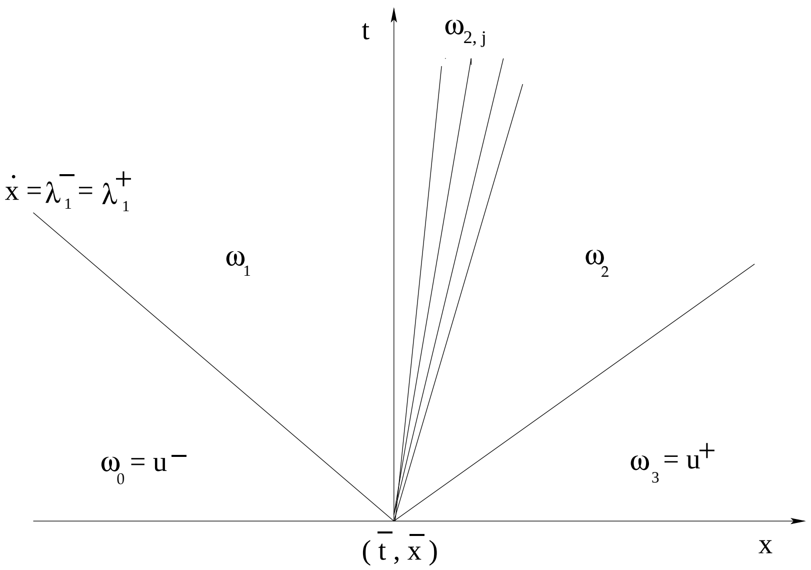

figure 17

Let $\delta > 0$ be a fixed small constant. If the i-th characteristic field is genuinely nonlinear and $\sigma_i > 0$, consider the integer

$$p_i \doteq 1 + [\![\sigma_i/\delta]\!], \tag{2.15}$$

where $[\![s]\!]$ denotes the integer part of s, i.e. the largest integer $\leq s$. For $j = 1, \ldots, p_i$, define

$$\omega_{i,j} = \Psi_i(j\sigma_i/p_i)(\omega_{i-1}), \qquad x_{i,j}(t) = \bar{x} + (t - \bar{t})\lambda_i(\omega_{i,j}). \tag{2.16}$$

On the other hand, if the i-th characteristic field is genuinely nonlinear and $\sigma_i \leq 0$, or if the i-th characteristic field is linearly degenerate (with σ_i arbitrary), define $p_i \doteq 1$ and

$$\omega_{i,1} = \omega_i, \qquad x_{i,1}(t) = \bar{x} + (t - \bar{t})\lambda_i(\omega_{i-1}, \omega_i). \tag{2.17}$$

Here $\lambda_i(\omega_{i-1},\omega_i)$ is the Rankine-Hugoniot speed of a jump connecting ω_{i-1} with ω_i, so that

$$\lambda(\omega_{i-1},\omega_i)\cdot\big(\omega_i-\omega_{i-1}\big)=f(\omega_i)-f(\omega_{i-1}). \tag{2.18}$$

As soon as the intermediate states $\omega_{i,j}$ and the locations $x_{i,j}(t)$ of the jumps have been determined by (2.16) and (2.17), we can define an approximate solution to the Riemann problem (2.11) by setting (fig. 17)

$$v(t,x)=\begin{cases} u^- & \text{if } \ x<x_{1,1}(t),\\ u^+ & \text{if } \ x>x_{n,p_n}(t),\\ \omega_i \ \ (=\omega_{i,p_i}) & \text{if } \ x_{i,p_i}(t)<x<x_{i+1,1}(t),\\ \omega_{i,j} & \text{if } \ x_{i,j}(t)<x<x_{i,j+1}(t) \qquad (j=1,\ldots,p_i-1). \end{cases} \tag{2.19}$$

Observe that the difference between v and the exact self-similar solution of (2.11) is due to the fact that every centered i-rarefaction wave is here divided into equal parts and replaced by a rarefaction fan containing p_i wave-fronts. Because of (2.15), the strength of each one of these fronts is $<\delta$.

Simplified Riemann Solver.

CASE 1: Let $j,j'\in\{1,\ldots,n\}$ be the families of the two incoming wave-fronts, with $j\geq j'$. Assume that the left, middle and right states u_l,u_m,u_r before the interaction are related by

$$u_m=\Psi_j(\sigma)(u_l),\qquad\qquad u_r=\Psi_{j'}(\sigma')(u_m). \tag{2.20}$$

Define the auxiliary right state

$$\tilde u_r=\begin{cases}\Psi_j(\sigma)\circ\Psi_{j'}(\sigma')(u_l) & \text{if } \ j>j',\\ \Psi_j(\sigma+\sigma')(u_r) & \text{if } \ j=j'.\end{cases} \tag{2.21}$$

Let $\tilde v=\tilde v(t,x)$ be the piecewise constant solution of the Riemann problem with data $u_l,\tilde u_r$, constructed as in (1.19). Because of (2.21), the piecewise constant function $\tilde v$ contains exactly two wave-fronts of sizes σ',σ, if $j>j'$, or a single wave-front of size $\sigma+\sigma'$, if $j=j'$.

Of course, in general one has $\tilde u_r\neq u_r$. We let the jump $(\tilde u_r,\ u_r)$ travel with a fixed speed $\hat\lambda$, strictly bigger than all characteristic speeds. In a forward neighborhood of the point $(\bar t,\bar x)$, we thus define an approximate solution v as follows (fig. 18a-b)

$$v(t,x)=\begin{cases}\tilde v(t,x) & \text{if} \quad x-\bar x<(t-\bar t)\hat\lambda,\\ u_r & \text{if} \quad x-\bar x>(t-\bar t)\hat\lambda.\end{cases} \tag{2.22}$$

Observe that this simplified Riemann solver introduces a new *non-physical* wave-front, travelling with constant speed $\hat{\lambda}$. In turn, this front may interact with other (physical) fronts. One more case of interaction thus needs to be considered.

CASE 2: A non-physical front hits from the left a wave-front of the i-characteristic family (fig. 18c), for some $i \in \{1, \ldots, n\}$.

Let u_l, u_m, u_r be the left, middle and right state before the interaction. If

$$u_r = \Psi_i(\sigma)(u_m), \tag{2.23}$$

define the auxiliary right state

$$\tilde{u}_r = \Psi_i(\sigma)(u_l). \tag{2.24}$$

Call $\tilde{v}$ the solution to the Riemann problem with data $u_l, \tilde{u}_r$, constructed as in (2.19). Because of (2.24), $\tilde{v}$ will contain a single wave-front belonging to the i-th family, with size σ. Since $\tilde{u}_r \neq u_r$ in general, we let the jump $(\tilde{u}_r,\ u_r)$ travel with the fixed speed $\hat{\lambda}$. In a forward neighborhood of the point $(\bar{t}, \bar{x})$, the approximate solution u is thus defined again according to (2.22).

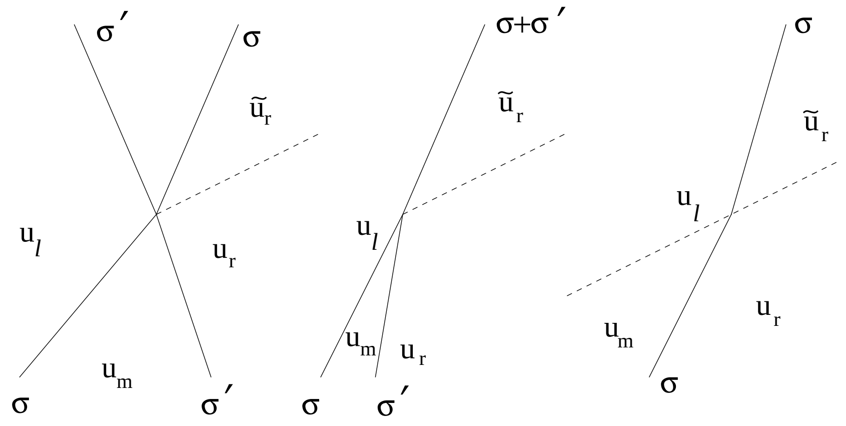

figure 18a figure 18b figure 18c

By construction, all non-physical fronts travel with the same speed $\hat{\lambda}$, hence they never interact with each other. The above cases therefore cover all possible interactions between two wave-fronts.

To complete the description of the algorithm, it remains to specify which Riemann solver is used at any given interaction. The choice is made in connection with a threshold parameter $\rho > 0$:

- The accurate method is used at time $t = 0$, and at every interaction where the product of the strengths of the incoming waves is $|\sigma\sigma'| \geq \rho$.
- The simplified method is used at every interaction involving a non-physical wave-front, and also at interactions where the product of the strengths of the incoming waves is $|\sigma\sigma'| < \rho$.

In the above, we tacitly assumed that only two wave-fronts interact at any given point. This can always be achieved by an arbitrarily small change in the speed of one of the interacting fronts. We shall also adopt the provision that, in the Accurate Riemann Solver, rarefaction fronts of the same family of one of the incoming fronts are never partitioned (even if their strength is $> \delta$). This guarantees that every wave-front can be uniquely continued forward in time, unless it gets completely cancelled by interacting with another front of the same family and opposite sign.

The construction of an approximate solution thus involves three parameters:

- A fixed speed $\hat{\lambda}$, strictly larger than all characteristic speeds.
- A small constant $\delta > 0$, controlling the maximum strength of rarefaction fronts.
- A threshold parameter $\rho > 0$, determining whether the Accurate or the Simplified Riemann Solver is used.

This completes the description of our algorithm. To prove Theorem 3, we now need to show that for any $\varepsilon > 0$, if the initial data $\bar{u}$ has small total variation, by a suitable choice of the parameters δ, ρ our algorithm will produce an ε-approximate solution defined for all $t \geq 0$. Observe that one can always solve the new Riemann problems generated by wave-front interactions provided that the states u^-, u^+ are close to each other. A key part of the proof will thus consist in showing that the total variation of the approximate solution remains small for all times. An outline of the proof is given below.

1. Interaction Estimates. Whenever two wave-fronts interact, the new Riemann problem is solved in terms of a family of outgoing waves. Well known estimates [15, 24] state that the difference between the strengths of the corresponding incoming and outgoing fronts is of second order. More precisely, the following holds.

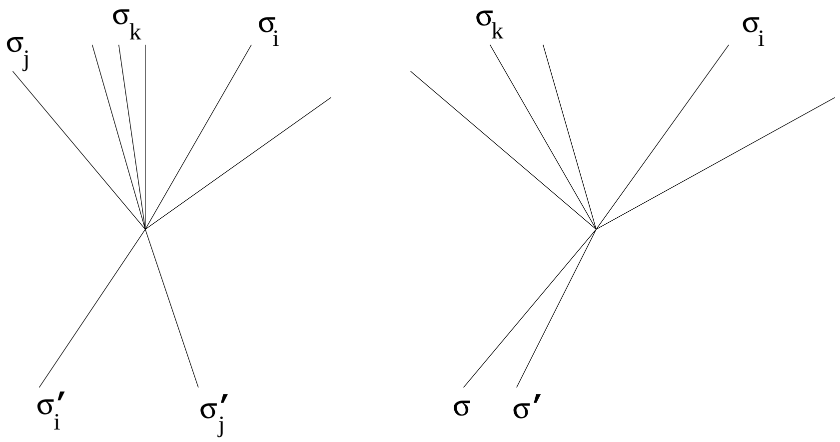

figure 19a   figure 19b

(i) Let σ_i, σ_j be the sizes of two incoming fronts, belonging to the distinct characteristic families $i > j$. Their interaction determines a Riemann problem (fig. 19a), whose solution consists of outgoing waves say of sizes $\sigma_1^+, \ldots, \sigma_n^+$. These are related to the incoming waves by the estimate

$$|\sigma_i^+ - \sigma_i| + |\sigma_j^+ - \sigma_j| + \sum_{k \neq i,j} |\sigma_k^+| = \mathcal{O}(1) \cdot |\sigma_i \sigma_j| \tag{2.25}$$

(ii) Let σ, σ' be the sizes of two incoming fronts, both belonging to the i-th characteristic family. As before, calling $\sigma_1^+, \ldots, \sigma_n^+$ the sizes of the outgoing waves generated by the corresponding Riemann problem (fig. 19b), one has

$$|\sigma_i^+ - \sigma - \sigma'| + \sum_{k \neq i} |\sigma_k^+| = \mathcal{O}(1) \cdot |\sigma\sigma'| \big(|\sigma| + |\sigma'|\big) \tag{2.26}$$

(iii) Let σ, σ' be the sizes of two incoming fronts, say of the families i, i'. Let u_l, u_m, u_r be the left, middle and right states before interaction, so that (2.20) holds. Introducing the auxiliary right state $\tilde{u}_r$ as in (2.21), one has (fig. 18a-b)

$$|\tilde{u}_r - u_r| = \mathcal{O}(1) \cdot |\sigma\sigma'|. \tag{2.27}$$

(iv) Let a non-physical front connecting the states u_l, u_m interact with an i-wave of size σ, connecting u_m, u_r, so that (1.13) holds. Defining the auxiliary right state $\tilde{u}_r$ as in (2.24), one has (fig. 18c)

$$|\tilde{u}_r - u_r| = \mathcal{O}(1) \cdot |\sigma| \big|u_m - u_l\big|. \tag{2.28}$$

2. Bounds on the Total Variation. These a priori bounds are derived from the above estimates (2.25)–(2.28), using an interaction functional introduced in [15]. Let $u = u(t, x)$ be a piecewise constant approximate solution. At a fixed time t let x_α, $\alpha = 1, \ldots, N$, be the locations of the fronts in $u(t, \cdot)$. Moreover, let $|\sigma_\alpha|$ be the strength of the wave-front at x_α. In case of a non-physical front, one simply defines

$$|\sigma_\alpha| \doteq \big|u(t, x_\alpha+) - u(t, x_\alpha-)\big|. \tag{2.29}$$

In the following, for notational convenience we say that non-physical fronts belong to a $(n+1)$-th characteristic family.

As in [15], consider the two functionals

$$V(t) \doteq \sum_\alpha |\sigma_\alpha|, \tag{2.30}$$

measuring the *total strength of waves* in $u(t, \cdot)$, and

$$Q(t) \doteq \sum_{(\alpha,\beta) \in \mathcal{A}} |\sigma_\alpha \sigma_\beta| \tag{2.31}$$

measuring the *wave interaction potential.* In (2.31), the summation ranges over all couples of approaching wave-fronts. More precisely, we say that two fronts, located at points $x_\alpha < x_\beta$ and belonging to the characteristic families $k_\alpha, k_\beta \in \{1, \ldots, n+1\}$ respectively, are *approaching* if $k_\alpha > k_\beta$ or else if $k_\alpha = k_\beta$ and at least one of the waves is a genuinely nonlinear shock.

Now consider any approximate solution constructed by the front tracking algorithm. At every time τ where two fronts of strength $|\sigma|, |\sigma'|$ interact, the interaction estimates (2.25)–(2.28) yield

$$V(\tau+) - V(\tau-) = \mathcal{O}(1) \cdot |\sigma\sigma'|, \tag{2.32}$$

$$Q(\tau+) - Q(\tau-) = -|\sigma\sigma'| + \mathcal{O}(1) \cdot |\sigma\sigma'| \cdot V(\tau-). \tag{2.33}$$

Indeed, the two fronts σ, σ' are no longer approaching after time τ. If V remains sufficiently small, (2.33) implies

$$Q(\tau+) - Q(\tau-) \leq -\frac{|\sigma\sigma'|}{2}. \tag{2.34}$$

By (2.34) and (2.32) we can thus choose a constant C_0 large enough so that the quantity

$$\Upsilon(t) \doteq V(t) + C_0 Q(t)$$

decreases at every interaction time, provided that V remains sufficiently small. Observing that

$$V(t) = \mathcal{O}(1) \cdot \text{Tot.Var.}\{u(t,\cdot)\}, \qquad Q(t) \leq V^2(t), \tag{2.35}$$

we conclude that, if the total variation of the initial data $u(0,\cdot)$ is sufficiently small, then

$$V(t) + C_0 Q(t) \leq V(0) + C_0 Q(0) \qquad \text{for all} \ \ t \geq 0. \tag{2.36}$$

By (2.35), the total variation of $u(t,\cdot)$ thus remains small for all times $t \geq 0$. In particular, the approximate solutions of all Riemann problems generated by the interactions are well defined.

3. Bounds on the number of wave fronts. To prove that the total number of wave fronts remains finite, we recall that the Accurate Riemann Solver is used when the strengths of the interacting waves satisfy $|\sigma\sigma'| \geq \rho$. This can happen only finitely many times. Indeed, by (2.34) at such times one has

$$Q(\tau+) - Q(\tau-) \leq -\rho/2. \tag{2.37}$$

Therefore, new physical fronts are introduced only at a number $\leq 2Q(0)/\rho$ of interaction points, hence their total number is finite. In turn, a new non-physical front is generated only when two physical fronts interact. Clearly, any two physical fronts can cross only once. Hence the total number of non-physical fronts is also finite.

The above steps **1**–**3** show that, for small enough initial data, the piecewise constant approximate solution is well defined for all times $t \geq 0$.

4. Strength of each rarefaction front is small. By construction, at a time t_0 where a new rarefaction front is introduced by the Accurate Riemann Solver, its size is $\sigma(t_0) \in]0, \delta]$. Observe that two rarefaction fronts of the same family never interact. If a rarefaction hits a shock of the same family, its size will decrease due to a cancellation. On the other hand, by subsequent interactions with fronts of other families, a rarefaction front may increase its initial strength. However, using the interaction estimates (2.25), it is not difficult to show that this strength remains uniformly bounded:

$$\sigma(t) = \mathcal{O}(1) \cdot \sigma(t_0) = \mathcal{O}(1) \cdot \delta \qquad \text{for all } t \geq t_0. \tag{2.38}$$

Choosing $\delta > 0$ sufficiently small, the right hand side of (2.38) remains smaller than ε.

5. Total strength of non-physical fronts is small. Toward this estimate, to each wave-front in u we attach an integer number, counting how many interactions were needed to produce such front. More precisely, the *generation order* of a front is inductively defined as follows (fig. 20).

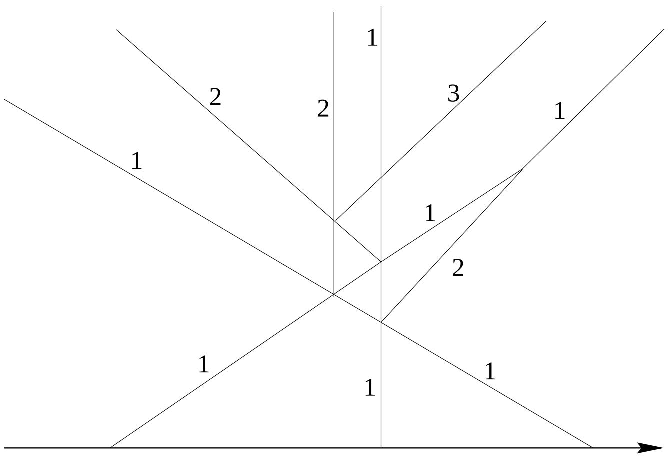

figure 20

- All fronts generated by the Riemann problems at the initial time $t = 0$ have generation order $k = 1$.
- Let two incoming fronts interact, say of the families $i, i' \in \{1, \dots, n+1\}$, with generation orders k, k'. The orders of the outgoing fronts are then defined as follows.

CASE 1: $i \neq i'$. Then

- the outgoing i-wave and i'-wave have the same orders k, k' as the incoming ones.
- the outgoing fronts of every other family $j \neq i, i'$ have order $\max\{k, k'\} + 1$.

CASE 2: $i = i'$. Then

- the outgoing front of the i-th family has order $\min\{k, k'\}$,

- the outgoing fronts of every family $j \neq i$ have order $\max\{k, k'\} + 1$.

For $k \geq 1$, call $V_k(t)$ the sum at time t of the strengths of all waves of order $\geq k$. Moreover set $Q_k(t) = \sum |\sigma_\alpha \sigma_\beta|$, where the sum extends over all couples of approaching waves in $u(t, \cdot)$, say of order k_α, k_β, with $\max\{k_\alpha, k_\beta\} \geq k$. If the total variation is sufficiently small, from the interaction estimates (2.25)–(2.28) one obtains the a priori bounds

$$V_k(t) \leq C\gamma^k \qquad \text{for all } \ t > 0, \ k \geq 1, \tag{2.39}$$

for some constants C and $\gamma < 1$. Now let N be the number of wave-fronts in $u(0+, \cdot)$. At any time $t > 0$, the number of first order fronts in $u(t, \cdot)$ is thus $\leq N$. From each interaction between fronts of first order, recalling that rarefaction waves are partitioned into pieces of size $< \delta$, a number $\mathcal{O}(1) \cdot 1/\delta$ of fronts of second order is generated. The total number of second order fronts is thus $\mathcal{O}(1) \cdot N^2/\delta$. By induction, the total number of fronts of order $\leq k$ in $u(t, \cdot)$ can be estimated by some polynomial function of N, δ^{-1}, say

$$[\text{number of fronts of order } \leq k] \leq P_k(N, \delta^{-1}). \tag{2.40}$$

The particular form of P_k is of no interest here. By the interaction estimate (2.27), if at some time t_0 the Simplified Riemann Solver introduces a new non-physical front, the strength of this new front is

$$\big|\sigma(t_0)\big| = \mathcal{O}(1) \cdot |\sigma\sigma'| = \mathcal{O}(1) \cdot \rho. \tag{2.41}$$

By subsequent interactions, the strength of a non-physical front may increase. However, using the estimates (2.28), one can show that this strength remains uniformly bounded:

$$\big|\sigma(t)\big| = \mathcal{O}(1) \cdot \big|\sigma(t_0)\big| = \mathcal{O}(1) \cdot \rho \qquad \text{for all } t \geq t_0.$$

Therefore

$$\big[\text{maximum strength of each non-physical front in } u\big] \leq C'\rho \tag{2.42}$$

for some constant C'. To estimate the total strength of all non-physical waves in $u(t, \cdot)$ we keep track of the fronts having generation order $> k$ and $\leq k$ separately. Using (2.39), (2.40) and (2.42) we deduce

$$\begin{aligned}
&\big[\text{total strength of non-physical fronts in } u(t, \cdot)\big] \\
&\qquad = \sum_{\text{order}(\alpha) > k} \big|\sigma_\alpha(t)\big| + \sum_{\text{order}(\alpha) \leq k} \big|\sigma_\alpha(t)\big| \\
&\qquad \leq \big[\text{total strength of all fronts of order } > k\big] \\
&\qquad\qquad + \big[\text{maximum strength of non-physical fronts}\big] \cdot \big[\text{number of fronts of order } \leq k\big] \\
&\qquad \leq C\gamma^k + C'\rho \cdot P_k(N, \delta^{-1}).
\end{aligned} \tag{2.43}$$

For any given $\varepsilon > 0$, since $\gamma < 1$ we can now choose k large enough so that $C\gamma^k < \varepsilon/2$. We then choose $\rho > 0$ small enough so that the second term on the right hand side of (2.43) is $< \varepsilon/2$. For all $t \geq 0$, this achieves

$$\big[\text{total strength of all non-physical fronts in } u(t,\cdot)\big] < \varepsilon, \tag{2.44}$$

completing the proof of Theorem 3.

We now work toward a proof of Theorem 2. Fix any sequence ε_ν decreasing to zero. For every $\nu \geq 1$, Theorem 3 yields the existence of an ε_ν-approximate solution u_ν of the Cauchy problem (2.1)-(2.2). By the previous analysis, these u_ν have uniformly bounded total variation. Moreover, the maps $t \mapsto u_\nu(t,\cdot)$ are uniformly Lipschitz continuous with values in $\mathbf{L}^1(I\!R;\ I\!R^n)$. Indeed,

$$\begin{aligned} \big\|u_\nu(t) - u_\nu(s)\big\|_{\mathbf{L}^1} &\leq (t-s)\cdot[\text{total strength of all wave fronts}]\cdot[\text{maximum speed}] \\ &\leq L\cdot(t-s) \end{aligned} \tag{2.45}$$

for some constant L independent of ν. We can thus apply Helly's compactness theorem and extract a subsequence which converges to some limit function u in $\mathbf{L}^1_{loc}$.

Since $\big\|u_\nu(0) - \bar u\big\|_{\mathbf{L}^1} \to 0$, by (2.45) the condition (2.2) clearly holds.

To prove that u is a weak solution of the Cauchy problem, it remains to show that, for every $\phi \in \mathcal{C}^1$ with compact support contained in the open half plane where $t > 0$, one has

$$\int_0^\infty \int_{-\infty}^\infty \phi_t(t,x)u(t,x) + \phi_x(t,x)f(u(t,x))\ dxdt = 0. \tag{2.46}$$

Since the u_ν are uniformly bounded and f is uniformly continuous on bounded sets, it suffices to prove that

$$\lim_{\nu\to 0}\left[\int_0^\infty\int_{-\infty}^\infty \Big\{\phi_t(t,x)u_\nu(t,x) + \phi_x(t,x)f\big(u_\nu(t,x)\big)\Big\}\ dxdt\right] = 0. \tag{2.47}$$

Choose $T > 0$ such that $\phi(t,x) = 0$ whenever $t \notin\,]0,T[$. For a fixed ν, at any time t call $x_1(t) < \cdots < x_N(t)$ the points where $u_\nu(t,\cdot)$ has a jump, and set

$$\Delta u_\nu(t,x_\alpha) \doteq u_\nu(t,x_\alpha+) - u_\nu(t,x_\alpha-), \qquad \Delta f\big(u_\nu(t,x_\alpha)\big) \doteq f\big(u_\nu(t,x_\alpha+)\big) - f\big(u_\nu(t,x_\alpha-)\big).$$

Observe that the polygonal lines $x = x_\alpha(t)$ subdivide the strip $[0,T]\times I\!R$ into finitely many regions Γ_j where u_ν is constant. Introducing the vector

$$\Phi \doteq \big(\phi\cdot u_\nu,\ \phi\cdot f(u_\nu)\big),$$

by the divergence theorem the double integral in (2.47) can be written as

$$\sum_j \iint_{\Gamma_j} \mathrm{div}\ \Phi(t,x)\,dtdx = \sum_j \int_{\partial\Gamma_j} \Phi\cdot\mathbf{n}\,d\sigma. \tag{2.48}$$

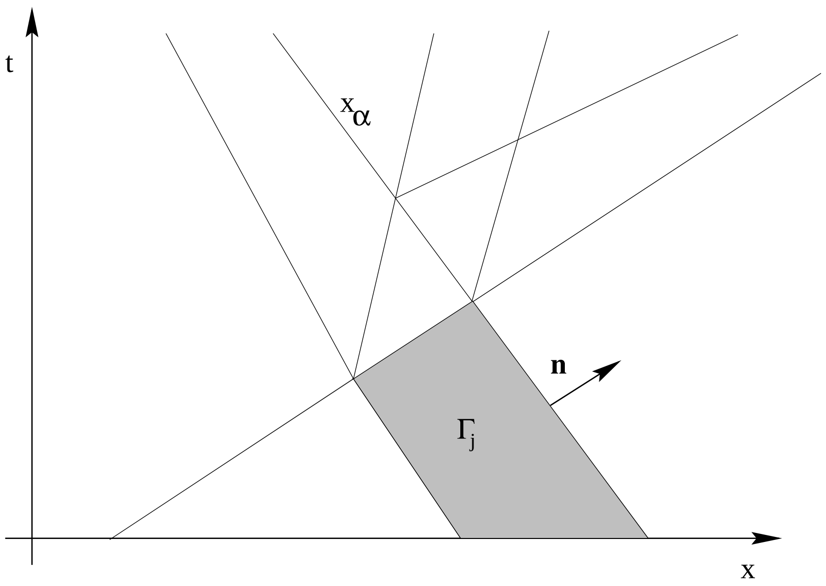

figure 21

Here $\partial\Gamma_j$ is the oriented boundary of Γ_j, while $\mathbf{n}$ denotes an outer normal (fig. 21). Observe that $\mathbf{n}d\sigma = \pm(\dot x_\alpha, -1)dt$ along each polygonal line $x = x_\alpha(t)$, while $\phi(t,x) = 0$ along the lines $t = 0, t = T$. By (2.48) the expression within square brackets in (2.47) is computed by

$$\int_0^T \sum_\alpha \Big[\dot x_\alpha(t)\cdot \Delta u_\nu(t,x_\alpha) - \Delta f\big(u_\nu(t,x_\alpha)\big)\Big]\phi\big(t,x_\alpha(t)\big)\ dt. \tag{2.49}$$

To estimate the above integral, let $|\sigma_\alpha|$ be the strength of the wave at x_α. If this wave is a shock, a rarefaction or contact discontinuity, by (2.4)–(2.7) one has

$$\Big|\dot x_\alpha(t)\cdot \Delta u_\nu(t,x_\alpha) - \Delta f\big(u_\nu(t,x_\alpha)\big)\Big| = \mathcal{O}(1)\cdot \varepsilon_\nu|\sigma_\alpha|. \tag{2.50}$$

On the other hand, if the wave at x_α is non-physical with strength $|\sigma_\alpha|$, then

$$\Big|\dot x_\alpha \cdot \Delta u_\nu(t,x_\alpha) - \Delta f\big(u_\nu(t,x_\alpha)\big)\Big| = \mathcal{O}(1)\cdot |\sigma_\alpha|. \tag{2.51}$$

We now split the summation in (2.49), considering physical (shocks, contacts or rarefactions) and nonphysical waves separately:

$$\begin{aligned}
&\limsup_{\nu\to\infty}\Bigg|\sum_{\alpha\in\mathcal{S}\cup\mathcal{R}\cup\mathcal{NP}}\Big[\dot x_\alpha(t)\cdot \Delta u_\nu(t,x_\alpha) - \Delta f\big(u_\nu(t,x_\alpha)\big)\Big]\phi\big(t,x_\alpha(t)\big)\Bigg|\\
&\quad\le \Big(\max_{t,x}\big|\phi(t,x)\big|\Big)\cdot \limsup_{\nu\to\infty}\Bigg\{\mathcal{O}(1)\cdot\sum_{\alpha\in\mathcal{S}\cup\mathcal{R}}\varepsilon_\nu|\sigma_\alpha| \ +\ \mathcal{O}(1)\cdot\sum_{\alpha\in\mathcal{NP}}|\sigma_\alpha|\Bigg\}\\
&\quad= 0.
\end{aligned} \tag{2.52}$$

Indeed, the total strength of waves in u_ν remains uniformly bounded, while the amount of non-physical waves by (2.44) approaches zero as $\varepsilon_\nu \to 0$. The limit (2.47) now follows from (2.52). Therefore, u is a weak solution to the Cauchy problem. In the presence of a convex entropy η with entropy flux q, an entirely similar argument shows that the inequality (1.26) is also satisfied.

3 - A semigroup of solutions.

The analysis in the previous chapter has shown the existence of a global entropy weak solution of the Cauchy problem for every initial data with sufficiently small total variation. More precisely, recalling the definitions (2.30)-(2.31), consider a domain of the form

$$\mathcal{D} = cl\Big\{u \in \mathbf{L}^1(\mathbb{R};\mathbb{R}^n);\quad u \text{ is piecewise constant},\quad \Upsilon(u) \doteq V(u) + C_0 \cdot Q(u) < \delta_0\Big\}, \tag{3.1}$$

where cl denotes closure in $\mathbf{L}^1$. With a suitable choice of the constants C_0 and $\delta_0 > 0$, the proofs of Theorems 2, 3 show that, for every $\bar u \in \mathcal{D}$, one can construct a sequence of ε-approximate front tracking solutions converging to a weak solution u taking values inside $\mathcal{D}$. Observe that, since the proof of convergence relied on a compactness argument, no information was obtained on the uniqueness of the limit. The main goal of the present chapter is to show that this limit is unique and depends continuously on the initial data:

Theorem 4. *For every $\bar u \in \mathcal{D}$, as $\varepsilon \to 0$ every sequence of ε-approximate solutions $u_\varepsilon : [0,\infty[\, \mapsto \mathcal{D}$ of the Cauchy problem (2.1)-(2.2) converges to a unique limit solution $u : [0,\infty[\, \mapsto \mathcal{D}$. The map $(\bar u, t) \mapsto u(t,\cdot) \doteq S_t \bar u$ is a uniformly Lipschitz semigroup, i.e.:*

$$S_0 \bar u = \bar u, \qquad S_s(S_t \bar u) = S_{s+t}\bar u, \tag{3.2}$$

$$\big\|S_t\bar u - S_s \bar v\big\|_{\mathbf{L}^1} \leq L \cdot \big(\|\bar u - \bar v\|_{\mathbf{L}^1} + |t-s|\big) \qquad \text{for all } \ \bar u, \bar v \in \mathcal{D}, \quad s,t \geq 0. \tag{3.3}$$

A construction of the semigroup was first carried out in [6] for 2×2 systems, then in [7] for general $n \times n$ systems. All these earlier estimates were based on a linearization + homothopy method. In order to estimate how the distance between two solutions u, v varies in time, one constructs a one-parameter family of solutions u^θ joining u with v, as shown in fig. 22. At any time $t \in [0,T]$, the distance $\big\|u(t) - v(t)\big\|_{\mathbf{L}^1}$ is thus bounded by the length of the curve $\gamma_t : \theta \mapsto u^\theta(t)$. In turn, as long as all solutions u^θ remain sufficiently regular, the length of γ_t can be computed by integrating the norm of a generalized tangent vector $\mathbf{v}$. The advantage of this approach is that tangent vectors satisfy a linearized evolution equation: a nonlinear problem is thus reduced to a family of linear problems. From a uniform a-priori estimate on the norm of these tangent vectors, one obtains a bound on the length of γ_T and hence on the distance between $u(T)$ and $v(T)$. Unfortunately, this approach is hampered by the possible loss of regularity of the solutions u^θ. In order to retain the minimal regularity (piecewise Lipschitz continuity) required for the existence of tangent vectors, in [6, 7] various approximation and restarting procedures had to be devised. These yield entirely rigorous proofs, but at the price of heavy technicalities.

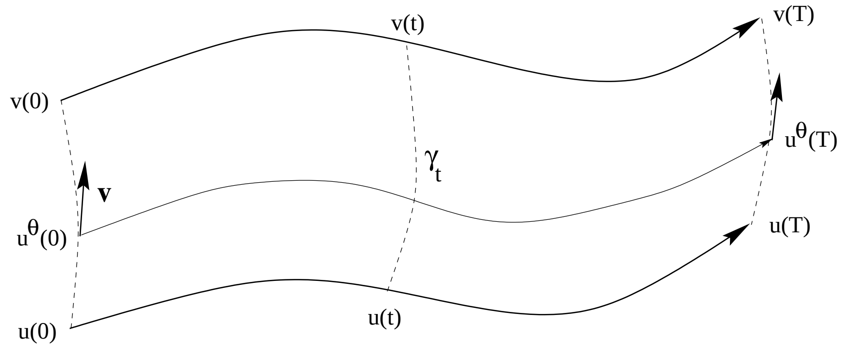

figure 22

In the remainder of this chapter, we will thus follow the new approach of Liu and Yang [19, 20] in its simplified version [11].

To prove the uniqueness of the limit of front tracking approximations, we need to estimate the distance between any two ε-approximate solutions u, v of (2.1). For this purpose, following [11] we introduce a functional $\Phi = \Phi(u, v)$, uniformly equivalent to the $\mathbf{L}^1$ distance, which is "almost decreasing" along pairs of solutions. Recalling the construction of shock curves at (1.39), given u, v, consider the scalar functions q_i defined implicitly by

$$v(x) = S_n\big(q_n(x)\big) \circ \ \cdots \ \circ S_1\big(q_1(x)\big)\big(u(x)\big). \tag{3.4}$$

Intuitively, $q_i(x)$ can be regarded as the strength of the i-shock wave in the jump $\big(u(x),\ v(x)\big)$. On a compact neighborhood of the origin, we clearly have

$$\frac{1}{C_1} \cdot \big|v(x) - u(x)\big| \leq \sum_{i=1}^{n} \big|q_i(x)\big| \leq C_1 \cdot \big|v(x) - u(x)\big| \tag{3.5}$$

for some constant C_1. We now consider the functional

$$\Phi(u, v) \doteq \sum_{i=1}^{n} \int_{-\infty}^{\infty} \big|q_i(x)\big| W_i(x)\ dx, \tag{3.6}$$

where the weights W_i are defined by setting:

$$\begin{aligned} W_i(x) &\doteq 1 + \kappa_1 \cdot \big[\text{total strength of waves in } u \text{ and in } v \text{ which approach the } i\text{-wave } q_i(x)\big] \\ &\qquad + \kappa_2 \cdot \big[\text{wave interaction potentials of } u \text{ and of } v\big] \\ &\doteq 1 + \kappa_1 A_i(x) + \kappa_2 \big[Q(u) + Q(v)\big]. \end{aligned} \tag{3.7}$$

The amount of waves approaching $q_i(x)$ is defined as follows. If the i-shock and i-rarefaction curves coincide, we simply take

$$A_i(x) \doteq \left[\sum_{x_\alpha < x, \ i < k_\alpha \leq n} + \sum_{x_\alpha > x, \ 1 \leq k_\alpha < i} \right] |\sigma_\alpha|. \tag{3.8}$$

The summations here extend to waves both of u and of v. According to [25], the definition (3.8) applies if the i-th field is linearly degenerate, or else if all i-rarefaction curves are straight lines. On the other hand, if the i-th field is genuinely nonlinear with shock and rarefactions curves not coinciding, our definition of A_i will contain an additional term, accounting for waves in u and in v of the same i-th family:

$$\begin{aligned} A_i(x) \doteq & \left[\sum_{\substack{\alpha \in \mathcal{J}(u) \cup \mathcal{J}(v) \\ x_\alpha < x, \ i < k_\alpha \leq n}} + \sum_{\substack{\alpha \in \mathcal{J}(u) \cup \mathcal{J}(v) \\ x_\alpha > x, \ 1 \leq k_\alpha < i}} \right] |\sigma_\alpha| \\ & + \begin{cases} \left[\displaystyle\sum_{\substack{k_\alpha = i \\ \alpha \in \mathcal{J}(u), \ x_\alpha < x}} + \sum_{\substack{k_\alpha = i \\ \alpha \in \mathcal{J}(v), \ x_\alpha > x}} \right] |\sigma_\alpha| & \text{if } \ q_i(x) < 0, \\ \left[\displaystyle\sum_{\substack{k_\alpha = i \\ \alpha \in \mathcal{J}(v), \ x_\alpha < x}} + \sum_{\substack{k_\alpha = i \\ \alpha \in \mathcal{J}(u), \ x_\alpha > x}} \right] |\sigma_\alpha| & \text{if } \ q_i(x) > 0. \end{cases} \end{aligned} \tag{3.9}$$

Here and in the sequel, $\mathcal{J}(u)$ and $\mathcal{J}(v)$ denote the sets of all jumps in u and in v, while $\mathcal{J} \doteq \mathcal{J}(u) \cup \mathcal{J}(v)$. We recall that $k_\alpha \in \{1, \ldots, n+1\}$ is the family of the jump located at x_α with size σ_α. Notice that the strengths of non-physical waves do enter in the definition of Q. Indeed, a non-physical front located at x_α approaches all shock and rarefaction fronts located at points $x_\beta > x_\alpha$. On the other hand, non-physical fronts play no role in the definition of A_i.

The values of the large constants κ_1, κ_2 in (3.7) will be specified later. Observe that, as soon as these constants have been assigned, we can then impose a suitably small bound on the total variation of u, v so that

$$1 \leq W_i(x) \leq 2 \qquad\qquad \text{for all } \ i, x. \tag{3.10}$$

From (3.5), (3.6) and (3.10) it thus follows

$$\frac{1}{C_1} \cdot \left\| v - u \right\|_{\mathbf{L}^1} \leq \Phi(u, v) \leq 2C_1 \cdot \left\| v - u \right\|_{\mathbf{L}^1}. \tag{3.11}$$

Recalling the definition $\Upsilon(u) \doteq V(u) + C_0 Q(u)$, the basic $\mathbf{L}^1$ stability estimate for front tracking approximations can now be stated as follows.

Theorem 5. *For suitable constants $C_2, \kappa_1, \kappa_2, \delta_0 > 0$ the following holds. Let u, v be ε-approximate front tracking solutions of (1.1) constructed by the algorithm in Chapter 2, with small total variation, so that*

$$\Upsilon\big(u(t)\big) < \delta_0, \qquad \Upsilon\big(v(t)\big) < \delta_0 \qquad \textit{for all } \ t \geq 0. \tag{3.12}$$

Then the functional Φ in (3.6)–(3.9) satisfies

$$\Phi\big(u(t),\ v(t)\big) - \Phi\big(u(s),\ v(s)\big) \leq C_2 \varepsilon (t-s) \qquad \textit{for all } \ 0 \leq s < t. \tag{3.13}$$

Relying on the above estimate, a proof of Theorem 4 can be easily worked out. Indeed, let $\bar u \in \mathcal{D}$ be given. Consider any sequence $\{u_\nu\}_{\nu \geq 1}$, such that each u_ν is a front tracking ε_ν-approximate solution of Cauchy problem (2.1)-(2.2), with

$$\lim_{\nu \to \infty} \varepsilon_\nu = 0, \qquad \Upsilon\big(u_\nu(t)\big) < \delta_0 \qquad \text{for all } t \geq 0,\ \nu \geq 1.$$

For every $\mu, \nu \geq 1$ and $t \geq 0$, by (3.11) and (3.13) it now follows

$$\begin{aligned} \big\| u_\mu(t) - u_\nu(t) \big\|_{\mathbf{L}^1} &\leq C_1 \cdot \Phi\big(u_\mu(t),\ u_\nu(t)\big) \\ &\leq C_1 \cdot \Big[\Phi\big(u_\mu(0),\ u_\nu(0)\big) + C_2 t \cdot \max\{\varepsilon_\mu,\ \varepsilon_\nu\} \Big] \\ &\leq 2C_1^2 \big\| u_\mu(0) - u_\nu(0) \big\|_{\mathbf{L}^1} + C_1 C_2 t \cdot \max\{\varepsilon_\mu,\ \varepsilon_\nu\}. \end{aligned} \tag{3.14}$$

Since the right hand side of (3.14) approaches zero as $\mu, \nu \to \infty$, the sequence is Cauchy and converges to a unique limit. The semigroup property (3.2) is an immediate consequence of uniqueness. Finally, let $\bar u, \bar v \in \mathcal{D}$ be given. For each $\nu \geq 1$, let u_ν, v_ν be front tracking ε_ν-approximate solutions of (2.1) with

$$\big\| u_\nu(0) - \bar u \big\|_{\mathbf{L}^1} < \varepsilon_\nu, \qquad \big\| v_\nu(0) - \bar v \big\|_{\mathbf{L}^1} < \varepsilon_\nu, \qquad \lim_{\nu \to \infty} \varepsilon_\nu = 0. \tag{3.15}$$

Using again (3.11) and (3.13) we deduce

$$\begin{aligned} \big\| u_\nu(t) - v_\nu(t) \big\|_{\mathbf{L}^1} &\leq C_1 \cdot \Phi\big(u_\nu(t),\ v_\nu(t)\big) \\ &\leq C_1 \cdot \Big[\Phi\big(u_\nu(0),\ v_\nu(0)\big) + C_2 t \varepsilon_\nu \Big] \\ &\leq 2C_1^2 \big\| u_\nu(0) - v_\nu(0) \big\|_{\mathbf{L}^1} + C_1 C_2 t \varepsilon_\nu. \end{aligned} \tag{3.16}$$

Letting $\nu \to \infty$, by (3.15) it follows

$$\big\| u(t) - v(t) \big\|_{\mathbf{L}^1} \leq 2C_1^2 \cdot \| \bar u - \bar v \|_{\mathbf{L}^1}. \tag{3.17}$$

This establishes the uniform Lipschitz continuity of the semigroup with respect to the initial data. Recalling (2.45), the Lipschitz continuity with respect to time is clear. This completes the proof of Theorem 4.

In the remainder of this chapter we will sketch the main ideas in the proof of Theorem 5. The key point is to understand how the functional Φ evolves in time. In connection with (3.4), at each x define the intermediate states $\omega_0(x) = u(x)$, $\omega_1(x)$, ... , $\omega_n(x) = v(x)$ by setting

$$\omega_i(x) \doteq S_i\big(q_i(x)\big) \circ \ S_{i-1}\big(q_{i-1}(x)\big) \circ \ \cdots \ \circ S_1\big(q_1(x)\big)\big(u(x)\big). \tag{3.18}$$

Moreover, call

$$\lambda_i(x) \doteq \lambda_i\big(\omega_{i-1}(x),\ \omega_i(x)\big) \tag{3.19}$$

the speed of the i-shock connecting $\omega_{i-1}(x)$ with $\omega_i(x)$. A direct computation now yields

$$\begin{aligned} \frac{d}{dt}\Phi\big(u(t),\ v(t)\big) &= \sum_{\alpha\in\mathcal{J}}\sum_{i=1}^n \Big\{\big|q_i(x_\alpha-)\big|W_i(x_\alpha-) - \big|q_i(x_\alpha+)\big|W_i(x_\alpha+)\Big\}\cdot \dot x_\alpha \\ &= \sum_{\alpha\in\mathcal{J}}\sum_{i=1}^n \Big\{\big|q_i^{\alpha+}\big|W_i^{\alpha+}\big(\lambda_i^{\alpha+} - \dot x_\alpha\big) - \big|q_i^{\alpha-}\big|W_i^{\alpha-}\big(\lambda_i^{\alpha-} - \dot x_\alpha\big)\Big\}, \end{aligned} \tag{3.20}$$

with obvious meaning of notations. We regard the quantity $\big|q_i(x)\big|\lambda_i(x)$ as the flux of the i-th component of $|v-u|$ at x. For $x_{\alpha-1} < x < x_\alpha$, one clearly has

$$\big|q_i^{(\alpha-1)+}\big|\,\lambda_i^{(\alpha-1)+}\,W_i^{(\alpha-1)+} = \big|q_i(x)\big|\lambda_i(x)W_i(x) = \big|q_i^{\alpha-}\big|\,\lambda_i^{\alpha-}\,W_i^{\alpha-}.$$

Moreover, the assumption $u(t), v(t) \in \mathbf{L}^1$ and piecewise constant implies $q_i(t,x) \equiv 0$ for x outside a bounded interval. This allowed us to add and subtract the above terms in (3.20), without changing the overall sum.

In connection with (3.20), for each jump point $\alpha \in \mathcal{J}$ and every $i = 1, \ldots, n$, define

$$E_{\alpha,i} \doteq \big|q_i^{\alpha+}\big|W_i^{\alpha+}\big(\lambda_i^{\alpha+} - \dot x_\alpha\big) - \big|q_i^{\alpha-}\big|W_i^{\alpha-}\big(\lambda_i^{\alpha-} - \dot x_\alpha\big). \tag{3.21}$$

Our main goal will be to establish the bounds

$$\sum_{i=1}^n E_{\alpha,i} \leq \mathcal{O}(1)\cdot|\sigma_\alpha| \qquad \alpha \in \mathcal{NP}, \tag{3.22}$$

$$\sum_{i=1}^n E_{\alpha,i} \leq \mathcal{O}(1)\cdot\varepsilon|\sigma_\alpha| \qquad \alpha \in \mathcal{R}\cup\mathcal{S}. \tag{3.23}$$

As usual, by the Landau symbol $\mathcal{O}(1)$ we denote a quantity whose absolute value satisfies a uniform bound, depending only on the system (2.1). In particular, this bound does not depend on ε or on the functions u, v. It is also independent of the choice of the constants κ_1, κ_2 in (3.7).

From (3.22)-(3.23), recalling (2.9) and the uniform bounds (3.12) on the total strength of waves, one obtains the key estimate

$$\frac{d}{dt}\Phi\big(u(t),\ v(t)\big) \leq \mathcal{O}(1)\cdot\varepsilon. \tag{3.24}$$

If the constant κ_2 in (3.7) is chosen large enough, by the interaction estimates (2.25)–(2.28) all weight functions $W_i(x)$ will decrease at each time τ where two fronts of u or two fronts of v interact. Integrating (3.24) over the interval $[s,t]$ we therefore obtain

$$\Phi\big(u(t),\ v(t)\big) \leq \Phi\big(u(s),\ v(s)\big) + \mathcal{O}(1)\cdot\varepsilon(t-s), \tag{3.25}$$

proving the theorem. All the remaining work is thus aimed at establishing (3.22)-(3.23).

If $\alpha \in \mathcal{NP}$, calling σ_α the strength of this jump as in (2.29), for $i = 1,\ldots,n$ one has the easy estimates

$$\begin{aligned} q_i^{\alpha+} - q_i^{\alpha-} &= \mathcal{O}(1)\cdot\sigma_\alpha,\\ \lambda_i^{\alpha+} - \lambda_i^{\alpha-} &= \mathcal{O}(1)\cdot\sigma_\alpha,\\ W_i^{\alpha+} - W_i^{\alpha-} &= 0 \qquad \text{if } \ q_i^{\alpha+}\cdot q_i^{\alpha-} > 0. \end{aligned}$$

Therefore, writing

$$\begin{aligned} E_{\alpha,i} = {} & \big(|q_i^{\alpha+}| - |q_i^{\alpha-}|\big)W_i^{\alpha+}(\lambda_i^{\alpha+} - \dot{x}_\alpha) \ + \ |q_i^{\alpha-}|(W_i^{\alpha+} - W_i^{\alpha-})(\lambda_i^{\alpha+} - \dot{x}_\alpha)\\ & + \ |q_i^{\alpha-}|W_i^{\alpha-}(\lambda_i^{\alpha+} - \lambda_i^{\alpha-}), \end{aligned} \tag{3.26}$$

the estimate (3.22) is clear.

The proof of (3.23) requires more work. Instead of writing down all computations, we will try to convey the main ideas with the help of a few pictures. For all details we refer to [11]. Given two piecewise constant functions u, v with compact support, for $i = 1,\ldots,n$ we can define the scalar components u_i, v_i as in [19], by induction on the jump points of u, v. We start by setting $u_i(-\infty) = v_i(-\infty) = 0$. If $x_\alpha \in \mathcal{J}(u)$ is a jump point of u, then we let v_i be constant across x_α and set

$$u_i(x_\alpha+) \doteq u_i(x_\alpha-) - \big[q_i(x_\alpha+) - q_i(x_\alpha-)\big].$$

On the other hand, if $x_\alpha \in \mathcal{J}(v)$ is a jump point of v, then we let u_i be constant across x_α and set

$$v_i(x_\alpha+) \doteq v_i(x_\alpha-) + \big[q_i(x_\alpha+) - q_i(x_\alpha-)\big].$$

These definitions trivially imply

$$q_i(x) = v_i(x) - u_i(x) \qquad\qquad \text{for all } \ x\in I\!R, \ \ i = 1,\ldots,n.$$

Observe that, according to the definition (3.9), the i-waves in u and v which approach $q_i(x)$ are those located within the thick portions of the graphs of u_i, v_i in fig. 23. Viceversa, for a given i-wave σ_α located at x_α, the regions where the jumps $q_i(x)$ approach σ_α are represented by the shaded areas in in fig. 24.

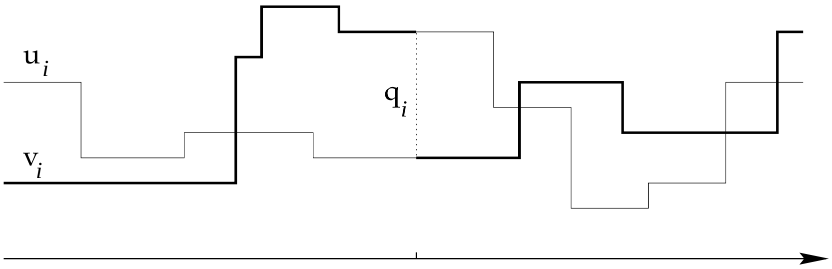

figure 23

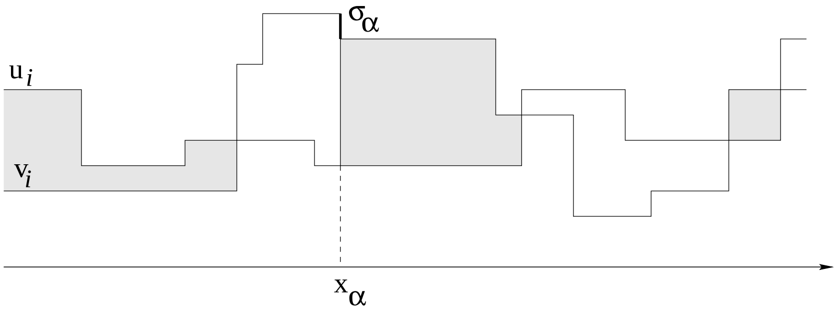

figure 24

Observe that the functional Φ in (3.6)-(3.7) can also be written in the equivalent form

$$\begin{aligned}\Phi(u,v) = \big[1+\kappa_2 Q(u)+\kappa_2 Q(v)\big]\cdot\sum_{i=1}^n\int_{-\infty}^{\infty}\big|q_i(x)\big|\,dx \\ +\kappa_1\cdot\sum_{\sigma_\alpha\in\mathcal{J}(u)\cup\mathcal{J}(v)}|\sigma_\alpha|\cdot\sum_i\int_{q_i(x)\text{approaches }\sigma_\alpha}\big|q_i(x)\big|\,dx\end{aligned}\tag{3.27}$$

Now let v have a wave-front at x_α with strength σ_α, in the genuinely nonlinear k-th family. To fix the ideas, assume that $v_k(x_\alpha\pm) > u_k(x_\alpha)$. In connection with this front, for every $i<k$ the functional $\Phi(u,v)$ in (3.27) contains a term of the form (fig. 25)

$$A_{\alpha,i}\doteq\kappa_1\cdot|\sigma_\alpha|\cdot\big[\text{area of the region between the graphs of } u_i \text{ and } v_i\text{, to the right of } x_\alpha\big].$$

By strict hyperbolicity, the i-th and k-th characteristic speeds are strictly separated, say $\lambda_k-\lambda_i\geq c>0$. If each component u_i,v_i, $i=1,\ldots,n$, were an exact solution to a scalar conservation law:

$$(u_i)_t+F_i(u_i)_x=0,\qquad\qquad (F_i'=\lambda_i)$$

uncoupled from all the other components, then we would have the estimate

$$\frac{dA_{\alpha,i}}{dt}\leq-\kappa_1|\sigma_\alpha|\big|q_i^{\alpha+}\big|(\dot x_\alpha-\lambda_i^{\alpha+})\leq-c\kappa_1|\sigma_\alpha|\big|q_i^{\alpha+}\big|.\tag{3.28}$$

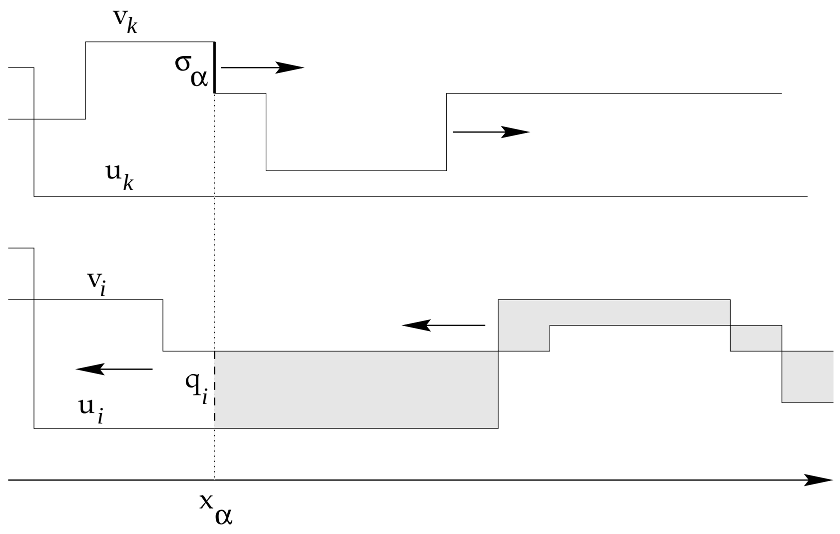

figure 25

Here $\lambda_i^{\alpha+} \doteq \lambda_i\big(u_i(x_\alpha+),\ v_i(x_\alpha+)\big)$ is a speed of an i-shock of strength $q_i^{\alpha+}$. In general, the estimate (3.28) must be supplemented with coupling and error terms, whose size is estimated as

$$\mathcal{O}(1)\cdot\left(\varepsilon+|q_k^{\alpha+}|\big(|q_k^{\alpha+}|+|\sigma_\alpha|\big)+\sum_{j\neq k}\big|q_j^{\alpha+}\big|\right)|\sigma_\alpha|. \tag{3.29}$$

A detailed computation thus yields

$$E_{\alpha,i}\leq\mathcal{O}(1)\cdot\left(\varepsilon+|q_k^{\alpha+}|\big(|q_k^{\alpha+}|+|\sigma_\alpha|\big)+\sum_{j\neq k}\big|q_j^{\alpha+}\big|\right)|\sigma_\alpha|-c\kappa_1\big|q_i^{\alpha+}\big||\sigma_\alpha| \qquad i\neq k. \tag{3.30}$$

Next, according to (3.9) the functional $\Phi(u,v)$ in (3.27) also contains a term of the form

$$A_{\alpha,k}\doteq\kappa_1\cdot|\sigma_\alpha|\cdot\big[\text{area of the region between the graphs of } u_k \text{ and } v_k\text{, to the right of } x_\alpha\big].$$

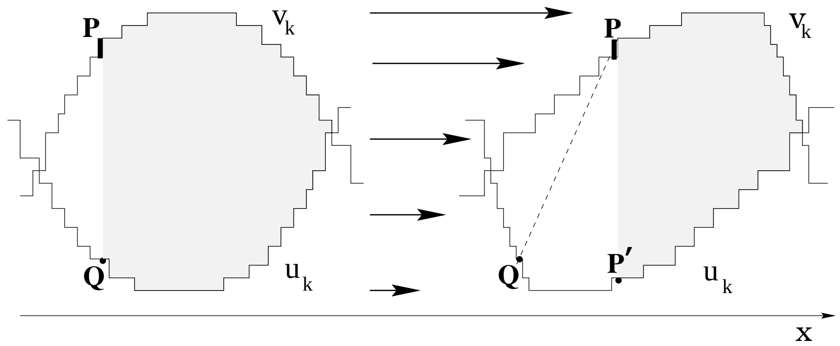

figure 26

If the components u_k, v_k were exact solutions of a genuinely nonlinear scalar conservation law, say

$$(u_k)_t + F_k(u_k)_x = 0, \qquad\qquad (F_k' = \lambda_k) \tag{3.31}$$

with $F_k'' \geq c' > 0$, then one would have the estimate

$$\frac{dA_{\alpha,k}}{dt} \leq -\kappa_1 |\sigma_\alpha| \big|q_k^{\alpha+}\big| (\dot x_\alpha - \lambda_k^{\alpha+}) \leq -\kappa_1 |\sigma_\alpha| \big|q_k^{\alpha+}\big| \cdot \frac{c'}{2} \big(|q_k^{\alpha+}| + |\sigma_\alpha|\big). \tag{3.32}$$

The decrease of this area is illustrated in fig. 26. In general, the estimate (3.32) must be supplemented with coupling and error terms, whose size is again estimated as (3.29). A detailed computation thus yields

$$E_{\alpha,k} \leq \mathcal{O}(1) \cdot \left(\varepsilon + |q_k^{\alpha+}| \big(|q_k^{\alpha+}| + |\sigma_\alpha|\big) + \sum_{j \neq k} \big|q_j^{\alpha+}\big| \right) |\sigma_\alpha| - \frac{c'\kappa_1}{2} |q_k^{\alpha+}| |\sigma_\alpha| \big(|q_k^{\alpha+}| + |\sigma_\alpha|\big). \tag{3.33}$$

Choosing κ_1 sufficiently large, (3.30) and (3.33) together yield (3.23).

A different estimate is needed in the case where the jump in v_k crosses the graph of u_k, say $v_k(x_\alpha+) < u_k(x_\alpha) < v_k(x_\alpha-)$. To fix the ideas, assume

$$\big|q_k^{\alpha+}\big| = \big|v_k(x_\alpha+) - u_k(x_\alpha)\big| \leq \big|v_k(x_\alpha-) - u_k(x_\alpha)\big| = \big|q_k^{\alpha-}\big|. \tag{3.34}$$

In this case, the estimates (3.30) remain valid. In connection with the k-th field, the functional Φ contains a term of the form (fig. 27):

$$A_{\alpha,k} \doteq \big[\text{area of the region between the graphs of } u_k \text{ and } v_k\big], \tag{3.35}$$

where the above area includes points both to the right and to the left of x_α.

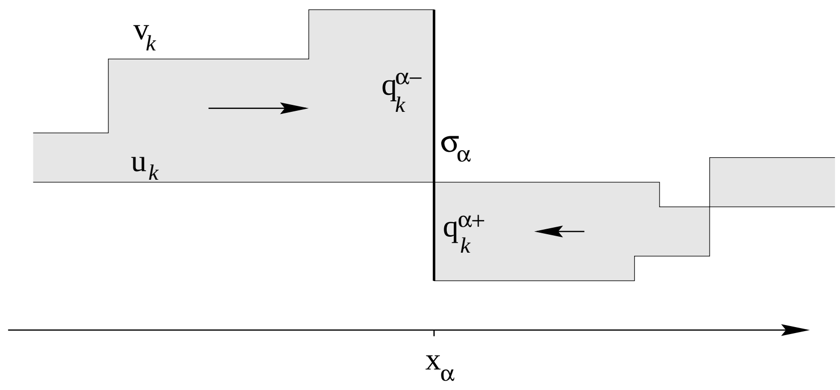

figure 27

If the components u_k, v_k provided an exact solution to the genuinely nonlinear scalar conservation law (3.31), due to genuine nonlinearity we would have

$$\frac{dA_{\alpha,k}}{dt} \leq -\frac{c'}{2}|q_k^{\alpha-}| \cdot |q_k^{\alpha+}| \leq -\frac{c'}{4}|\sigma_\alpha||q_k^{\alpha+}|. \tag{3.36}$$

Indeed, by (3.34),

$$|\sigma_\alpha| = |q_k^{\alpha-}| + |q_k^{\alpha+}| \leq 2|q_k^{\alpha-}|.$$

In general, the estimate (3.36) must be supplemented with coupling and error terms, whose size is again estimated as (3.29). A detailed computation thus yields

$$E_{\alpha,k} \leq \mathcal{O}(1) \cdot \left(\varepsilon + |q_k^{\alpha+}|\big(|q_k^{\alpha+}| + |\sigma_\alpha|\big) + \sum_{j \neq k} |q_j^{\alpha+}| \right) |\sigma_\alpha| - \frac{c'}{4}|q_k^{\alpha+}||\sigma_\alpha|. \tag{3.37}$$

Assuming that the total strength of waves remains sufficiently small, we have

$$|q_k^{\alpha+}| + |\sigma_\alpha| \ll \frac{c'}{4},$$

hence (3.30) and (3.37) together yield (3.23). For details we again refer to [11].

4 - Uniqueness of solutions.

According to the analysis in the previous chapters, the solution of the Cauchy problem (2.1)-(2.2) obtained as limit of front tracking approximations is unique and depends Lipschitz continuously on the initial data, in the $\mathbf{L}^1$ norm. This basic result, however, leaves open the question whether other weak solutions may exist, possibly constructed by different approximation algorithms. We will show that this is not the case: indeed, every entropy admissible solution, satisfying some minimal regularity assumptions, necessarily coincides with the one obtained as limit of front tracking approximations. Toward this result, a simple formula for estimating errors will be needed.

Lemma 1. *Let $S : \mathcal{D} \times [0, \infty \mapsto \mathcal{D}$ be a Lipschitz continuous semigroup, satisfying (3.2)-(3.3) for some constants L, L'. For any Lipschitz continuous map $u : [0,T] \mapsto \mathcal{D}$ one then has*

$$\big\|u(T) - S_T u(0)\big\|_{\mathbf{L}^1} \leq L \cdot \int_0^T \left\{ \liminf_{h \to 0+} \frac{\big\|u(t+h) - S_h u(t)\big\|_{\mathbf{L}^1}}{h} \right\} \, dt\,. \tag{4.1}$$

Observe that the integrand on the right hand side of (4.1) can be interpreted as an *instantaneous error rate*. As shown in fig. 28, the distance $\big\|u(T) - S_T u(0)\big\|_{\mathbf{L}^1}$ is bounded by the length

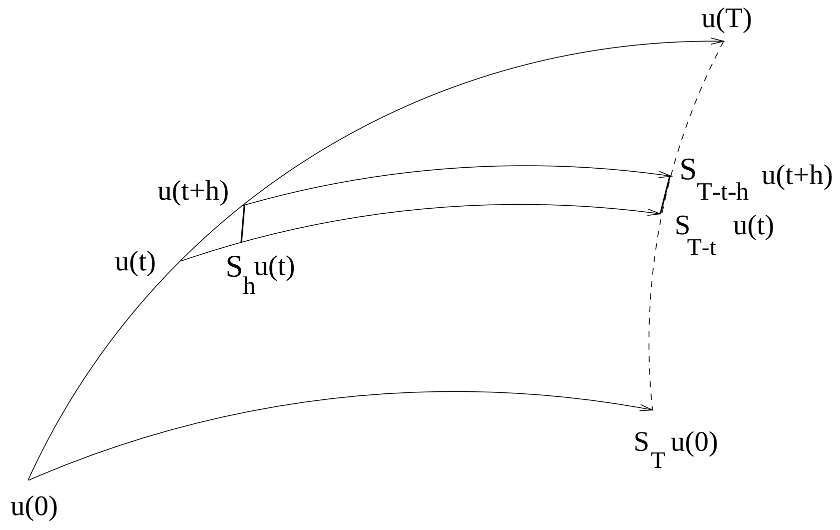

figure 28

of the path $t \mapsto S_{T-t}u(t)$. In turn, this length is obtained by integrating the instantaneous error rate, magnified by a factor L. Indeed

$$\big\|S_{T-(t+h)}u(t+h) - S_{T-t}u(t)\big\| \leq L \cdot \big\|u(t+h) - S_h u(t)\big\|.$$

For a detailed proof of (4.1), see [6, p.26].

As a first application of Lemma 1, let $t \mapsto u(t,\cdot) = S_t\bar{u}$ be the semigroup trajectory yielding the exact solution of the Cauchy problem (2.1)-(2.2). Let $u^\varepsilon : [0,T] \mapsto \mathcal{D}$ be an ε-approximate front tracking solution, according to Definition 2. We now show that the corresponding error can then be estimated as

$$\big\|u^\varepsilon(T,\cdot) - S_T\bar{u}\big\|_{\mathbf{L}^1} = \mathcal{O}(1) \cdot \varepsilon(1+T). \tag{4.2}$$

To see this, we first estimate the limit

$$\lim_{h\to 0+} \frac{\big\|u^\varepsilon(\tau+h) - S_h u^\varepsilon(\tau)\big\|_{\mathbf{L}^1}}{h}$$

at any time $\tau \in [0,T]$ where no wave-front interaction takes place. Let $u(\tau,\cdot)$ have jumps at points $x_1 < \cdots < x_N$. Call $\mathcal{S}$ the set of indices $\alpha \in \{1,\ldots,N\}$ such that $u(\tau, x_\alpha-)$ and $u(\tau, x_\alpha+)$ are connected by a shock or by a contact discontinuity, so that (2.4)-(2.5) hold. Moreover, call $\mathcal{R}$ the set of indices α corresponding to a rarefaction wave of a genuinely nonlinear family, so that (2.6)-(2.7) hold. Finally, call $\mathcal{NP}$ the set of indices α corresponding to non-physical fronts.
For each α, call ω_α the self-similar solution of the Riemann problem with data $u^\pm = u(\tau,\ x_\alpha\pm)$. We observe that, for $h > 0$ small enough, the semigroup trajectory $h \mapsto S_h u(\tau)$ is obtained by piecing together the solutions of these Riemann problems (fig. 29). Using the properties (2.4)–(2.9)

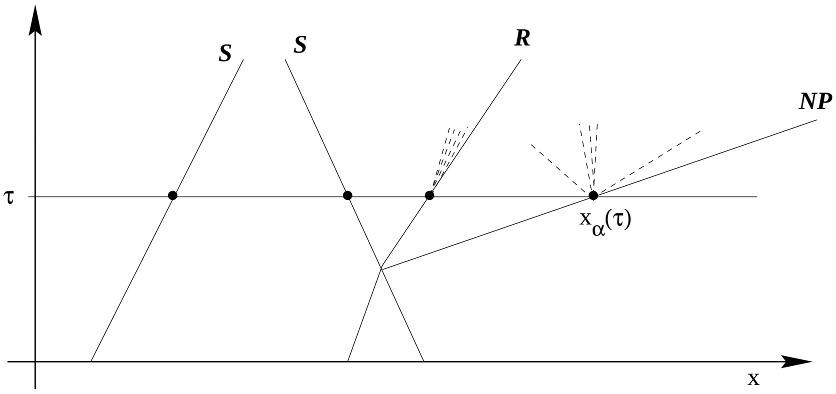

figure 29

one now derives the bound

$$\lim_{h\to 0+} \frac{\big\|u(\tau+h)-\widetilde S_h u(\tau)\big\|_{\mathbf{L}^1}}{h} = \sum_{\alpha\in\mathcal{R}\cup\mathcal{S}\cup\mathcal{NP}} \left(\lim_{h\to 0+}\frac{1}{h}\int_{x_\alpha-\rho}^{x_\alpha+\rho} \big|u(\tau+h,x)-\omega_\alpha(h,\ x-x_\alpha)\big|\ dx\right)$$
$$= \sum_{\alpha\in\mathcal{S}} \mathcal{O}(1)\cdot\varepsilon|\sigma_\alpha| + \sum_{\alpha\in\mathcal{R}} \mathcal{O}(1)\cdot|\sigma_\alpha|\big(|\sigma_\alpha|+\varepsilon\big) + \sum_{\alpha\in\mathcal{NP}} \mathcal{O}(1)\cdot|\sigma_\alpha|$$
$$= \mathcal{O}(1)\cdot\varepsilon\,. \tag{4.3}$$

Here ρ can be any suitably small positive number. From the assumption (2.10), the bound (4.3) and the error formula (4.1) we finally obtain

$$\begin{aligned}\big\|u^\varepsilon(T,\cdot)-S_T\bar u\big\|_{\mathbf{L}^1} &\le \big\|S_T u^\varepsilon(0,\cdot)-S_T\bar u\big\|_{\mathbf{L}^1} + \big\|u^\varepsilon(T,\cdot)-S_T u^\varepsilon(0,\cdot)\big\|_{\mathbf{L}^1}\\ &\le L\cdot\big\|u^\varepsilon(0,\cdot)-\bar u\big\|_{\mathbf{L}^1} + L\cdot\int_0^T\left\{\liminf_{h\to 0+}\frac{\big\|u^\varepsilon(\tau+h)-S_h u^\varepsilon(\tau)\big\|_{\mathbf{L}^1}}{h}\right\}d\tau\\ &= \mathcal{O}(1)\cdot\varepsilon+\mathcal{O}(1)\cdot\varepsilon T.\end{aligned}$$

We shall now state our main uniqueness theorem. For scalar conservation laws, a very general uniqueness and stability result was proved in the fundamental paper of Kruzhkov [17]. In the case of $n\times n$ systems, under some mild regularity assumptions, the uniqueness of entropy weak solutions with small total variation was recently proved in [8, 9, 10]. For sake of clarity, a complete set of assumptions is listed below.

(A1) **(Conservation Equations)** The function $u=u(t,x)$ is a weak solution of the Cauchy problem (2.1)-(2.2), taking values within the domain $\mathcal{D}$ of a semigroup S. More precisely, $u:[0,T]\mapsto\mathcal{D}$ is continuous w.r.t. the $\mathbf{L}^1$ distance. The initial condition (2.2) holds, together with

$$\iint \big(u\varphi_t+f(u)\varphi_x\big)\ dxdt = 0 \tag{4.4}$$

for every $\mathcal{C}^1$ function φ with compact support contained inside the open strip $]0,T[\times I\!\!R$.

(A2) **(Lax Entropy Condition)** Let u have an approximate jump discontinuity at some point $(\tau,\xi)\in]0,T[\times I\!\!R$. More precisely, let there exists states $u^-,u^+\in\Omega$ and a speed $\lambda\in I\!\!R$ such that, calling

$$U(t,x)\doteq\begin{cases}u^- & \text{if} \quad x<\lambda t,\\ u^+ & \text{if} \quad x>\lambda t,\end{cases}\tag{4.5}$$

there holds

$$\lim_{r\to 0+}\frac{1}{r^2}\int_{-r}^{r}\int_{-r}^{r}\Big|u(\tau+t,\ \xi+x)-U(t,x)\Big|\,dxdt=0.\tag{4.6}$$

Then, for some $i\in\{1,\ldots,n\}$, one has the inequalities

$$\lambda_i(u^-)\geq\lambda\geq\lambda_i(u^+).\tag{4.7}$$

(A3) **(Tame Oscillation Condition)** For some constants C, $\hat{\lambda}$ the following holds. For every point $x\in I\!\!R$ and every $t,h>0$ one has

$$\big|u(t+h,x)-u(t,x)\big|\leq C\cdot\text{Tot.Var.}\big\{u(t,\cdot);[x-\hat{\lambda}h,\ x+\hat{\lambda}h]\big\}.\tag{4.8}$$

(A4) **(Bounded Variation Condition)** There exists $\delta>0$ such that, for every space-like curve $\big\{t=\tau(x)\big\}$ with $|d\tau/dx|\leq\delta$ a.e., the function $x\mapsto u\big(\tau(x),x\big)$ has locally bounded variation.

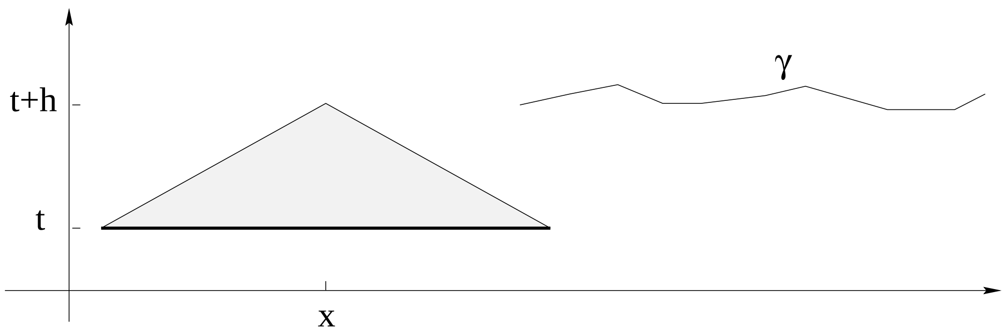

figure 30

Remark 1. The condition (A3) restricts the oscillation of the solution. An equivalent, more intuitive formulation is the following. For some constant $\hat{\lambda}$ larger than all characteristic speeds, given any interval $[a,b]$ and $t\geq 0$, the oscillation of u on the triangle (fig. 30) $\Delta\doteq\big\{(s,y):\quad s\geq t,\ a+\hat{\lambda}(s-t)<y<b-\hat{\lambda}(s-t)\big\}$, defined as

$$\text{Osc}\big\{u;\ \Delta\big\}\doteq\sup_{(s,y),(s',y')\in\Delta}\big|u(s,y)-u(s',y')\big|,$$

is bounded by a constant multiple of the total variation of $u(t,\cdot)$ on $[a,b]$.
Assumption (A4) simply requires that, for some fixed $\delta>0$, the function u has bounded variation along every space-like curve γ as in fig. 30, of the form $\big\{t=\tau(x);\ x\in[a,b]\big\}$ with slope $\leq\delta$, i.e. with

$$\big|\tau(x)-\tau(x')\big|\leq\delta|x-x'|\qquad\qquad\text{for all }\ x,x'\in[a,b].$$

One can prove that all of the above assumptions are satisfied by weak solutions obtained as limits of Glimm or wave-front tracking approximations [6, p.185]. The following result shows that the entropy weak solution of the Cauchy problem (2.1)-(2.2) is unique within the class of functions that satisfy either the additional regularity condition (A3), or (A4).

Theorem 6. *Let the map $u:[0,T]\mapsto\mathcal{D}$ be continuous (w.r.t. the $\mathbf{L}^1$ distance), taking values in the domain of the semigroup S generated by the system (2.1). If* (A1), (A2) *and* (A3) *hold, then*

$$u(t,\cdot)=S_t\bar u\qquad\qquad\textit{for all }\ t\in[0,T].\tag{4.9}$$

In particular, the weak solution that satisfies these conditions is unique. The same conclusion holds if the assumption (A3) *is replaced by* (A4).

The first part of Theorem 6 follows from the results in [8], the second part was proved in [10]. The main steps of the proof are given below. For more details see [6, p.188].

1. Since u takes values inside the domain $\mathcal{D}$ of the semigroup, the total variation of $u(t,\cdot)$ remains uniformly bounded. From the basic equation (2.1), it follows that u is Lipschitz continuous with values in $\mathbf{L}^1$, namely

$$\big\|u(t)-u(s)\big\|_{\mathbf{L}^1}\leq L\cdot|t-s|\tag{4.10}$$

for some Lipschitz constant L. More precisely, if M and λ^* are constants such that

$$\text{Tot.Var.}(u)\leq M\qquad\qquad\text{for all }\ u\in\mathcal{D},$$

$$\big|f(\omega)-f(\omega')\big|\leq\lambda^*|\omega-\omega'|\qquad\qquad\text{whenever }\ |\omega|,|\omega'|\leq M,$$

as Lipschitz constant in (4.10) one can take $L\doteq\lambda^*M$. As a consequence, $u=u(t,x)$ can be regarded as a BV function of the two variables t,x, in the sense that the distributional derivatives D_tu, D_xu are Radon measures. By a well known structure theorem [14], there exists a set $\widetilde{\mathcal{N}}\subset\,]0,T[\,\times I\!R$ of 1-dimensional Hausdorff measure zero such that, at every point $(\tau,\xi)\notin\widetilde{\mathcal{N}}$, u either is approximately continuous or has an approximate jump discontinuity. Taking the projection of $\widetilde{\mathcal{N}}$ on the t-axis, we conclude that there exists a set $\mathcal{N}\subset[0,T]$ of measure zero, containing the endpoints 0 and T, such that, at every point $(\tau,\xi)\in[0,T]\times I\!R$ with $\tau\notin\mathcal{N}$, setting $u^-\doteq u(\tau,\xi-)$, $u^+\doteq u(\tau,\xi+)$ the following property holds.

(P) Either $u^+ = u^-$, in which case (4.5)-(4.6) hold with λ arbitrary. Or else $u^+ \neq u^-$, in which case (4.5)-(4.6) hold for some particular $\lambda \in I\!R$. In this second case, for some $i \in \{1, \ldots, n\}$ the Rankine-Hugoniot equations and the Lax entropy condition hold:

$$\lambda_i(u^-, u^+) \cdot (u^+ - u^-) = f(u^+) - f(u^-), \qquad\qquad \lambda_i(u^+) \leq \lambda_i(u^-, u^+) \leq \lambda_i(u^-). \quad (4.11)$$

2. We will establish (4.9) by showing that the integrand on the right hand side of (4.1) vanishes at each time $t \notin \mathcal{N}$. Because of the finite speed of propagation, it actually suffices to show that, for each $t \notin \mathcal{N}$, $\varepsilon > 0$ and every interval $[a, b]$, there holds

$$\limsup_{h \to 0+} \frac{1}{h} \int_a^b \Big| u(t+h,\ x) - \big(S_h u(t)\big)(x) \Big|\, dx = \mathcal{O}(1) \cdot \varepsilon. \tag{4.12}$$

3. Let $u = u(t, x)$ be as in Theorem 6. In the following, for any given point (τ, ξ), we denote by $U^\sharp = U^\sharp_{(\tau,\xi)}$ the solution of the Riemann problem

$$w_t + f(w)_x = 0, \qquad\qquad w(\tau, x) = \begin{cases} u^+ \doteq u(\tau, \xi+) & \text{if} \quad x > \xi, \\ u^- \doteq u(\tau, \xi-) & \text{if} \quad x < \xi. \end{cases} \tag{4.13}$$

By the property (P), apart from the trivial case where $u^+ = u^-$, this solution consists of a single entropy admissible shock. The function $U^\sharp$ provides a good approximation to the solution u in a forward neighborhood of the point (τ, ξ). More precisely, using the Lipschitz continuity (4.10), one can prove that

$$\lim_{h \to 0+} \frac{1}{h} \int_{\xi - h\hat\lambda}^{\xi + h\hat\lambda} \Big| u(\tau + h,\ x) - U^\sharp_{(\tau,\xi)}(\tau + h,\ x) \Big|\, dx = 0, \tag{4.14}$$

for every $\hat\lambda > 0$ and every (τ, ξ) with $\tau \notin \mathcal{N}$.

4. Next, for a given point (τ, ξ) we denote by $U^\flat = U^\flat_{(\tau,\xi)}$ the solution of the linear system with constant coefficients

$$w_t + \widetilde{A} w_x = 0, \qquad\qquad w(\tau, x) = u(\tau, x), \tag{4.15}$$

where $\widetilde{A} \doteq A\big(u(\tau, \xi)\big)$. As in the previous step, we need to estimate the difference between u and $U^\flat$, in a forward neighborhood of the point (τ, ξ). Consider any open interval $]a, b[$ containing the point ξ and fix a speed $\hat\lambda$ strictly larger than the absolute values of all characteristic speeds. For $t \geq \tau$ define the open intervals

$$J(t) \doteq \ \big]a + (t - \tau)\hat\lambda, \quad b - (t - \tau)\hat\lambda\big[\tag{4.16}$$

and the region

$$\Gamma(t) \doteq \big\{(s, x); \quad s \in [\tau,\ t], \quad x \in J(s)\big\}. \tag{4.17}$$

With the above notation, for every $\tau' \geq \tau$ one can prove the estimate

$$\int_{J(\tau')} \left| u(\tau',\ x) - U^\flat(\tau',\ x) \right| dx = \mathcal{O}(1) \cdot \sup_{(t,x)\in\Gamma(\tau')} \left| u(t,x) - u(\tau,\xi) \right| \cdot \int_\tau^{\tau'} \text{Tot.Var.}\left\{ u(t,\cdot);\ J(t) \right\} dt. \tag{4.18}$$

5. Given $\tau \notin \mathcal{N}$, $\varepsilon > 0$ and $a < b$, using either one of the assumptions (A3) or (A4) we can cover a neighborhood of the interval $[a,b]$ with finitely many points ξ_i and open intervals $I_j \doteq]a_j,\ b_j[$ such that the following conditions hold (fig. 31).

(i) Each point x is contained in at most two of the open intervals I_j.

(ii) The total variation of $u(\tau,\cdot)$ on each I_j is $\leq \varepsilon$.

(iii) For some $\tau' > \tau$, calling $\zeta_j \doteq (a_j + b_j)/2$ and

$$\Gamma_j \doteq \left\{ (t,x);\quad t \in [\tau,\tau'],\quad a_j + (t-\tau)\hat\lambda \ <\ x\ <\ b_j - (t-\tau)\hat\lambda \right\},$$

there holds

$$\sup_{(t,x)\in\Gamma_j} \left| u(t,x) - u(\tau,\zeta_j) \right| \leq \varepsilon. \tag{4.19}$$

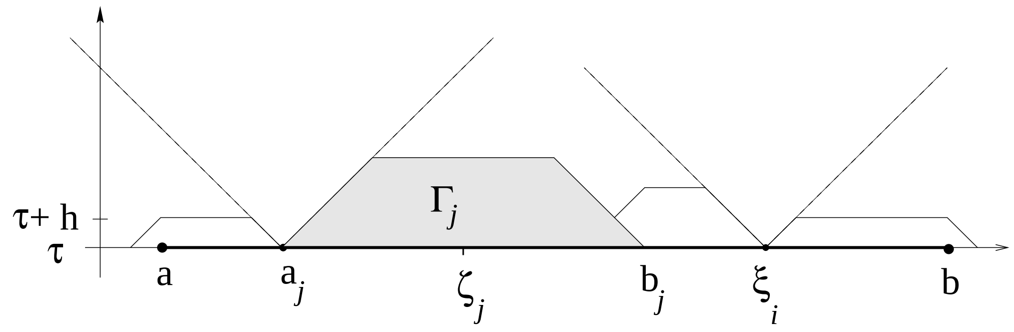

figure 31

6. We now construct a function $U = U(t,x)$ which coincides with $U^\sharp_{(\tau,\xi_i)}$ near each point (τ,ξ_i) and with $U^\flat_{(\tau,\zeta_j)}$ in a forward neighborhood of each point (τ,ζ_j).

$$U(t,x) \doteq \begin{cases} U^\sharp_{(\tau,\xi_i)}(t,x) & \text{if} \quad |x-\xi_i| \leq (t-\tau)\hat\lambda, \\ U^\flat_{(\tau,\zeta_j)}(t,x) & \text{if} \quad (t,x) \in \Gamma_j \setminus \bigcup_{k<j} \Gamma_k. \end{cases}$$

By (4.14) and (4.18), this function U provides a good approximation of u, for times $t = \tau + h$ with

$h > 0$ small. Indeed, recalling (4.19) and the property (i) of the covering, we have

$$
\begin{aligned}
&\limsup_{h\to 0+} \frac{1}{h}\int_a^b \Big|u(\tau+h,\ x) - U(\tau+h,\ x)\Big|\,dx \\
&\qquad \leq \sum_i \limsup_{h\to 0+} \frac{1}{h}\int_{\xi_i - h\hat\lambda}^{\xi_i + h\hat\lambda} \Big|u(\tau+h,\ x) - U^\sharp_{(\tau,\xi_i)}(\tau+h,\ x)\Big|\,dx \\
&\qquad\qquad + \sum_j \limsup_{h\to 0+} \frac{1}{h}\int_{a_j + h\hat\lambda}^{b_j - h\hat\lambda} \Big|u(\tau+h,\ x) - U^\flat_{(\tau,\zeta_j)}(\tau+h,\ x)\Big|\,dx \\
&\qquad \leq 0 + \limsup_{h\to 0+} \left\{ \mathcal{O}(1)\cdot \sum_j \frac{\varepsilon}{h}\int_\tau^{\tau+h} \text{Tot.Var.}\big\{u(t);\quad I_j\big\}\ dt \right\} \\
&\qquad \leq \limsup_{h\to 0+} \left\{ \mathcal{O}(1)\cdot \frac{\varepsilon}{h}\int_\tau^{\tau+h} 2\cdot \text{Tot.Var.}\big\{u(t);\quad I\!R\big\}\ dt \right\} \\
&\qquad = \mathcal{O}(1)\cdot\varepsilon.
\end{aligned}
\tag{4.20}
$$

7. We now observe that the semigroup trajectory $v(t,\cdot) \doteq S_t\bar u$ is also an entropy weak solution of the Cauchy problem (2.1)-(2.2), and satisfies all the assumptions (A1)–(A3). In particular, the total variation of $v(t,\cdot)$ remains uniformly bounded, and its oscillation on each domain $\Gamma(t)$ of the form (4.17) is bounded by

$$
\sup_{(t,x)\in\Gamma(\tau')} \Big|v(t,x) - v(\tau,\xi)\Big| = \mathcal{O}(1)\cdot \text{Tot.Var.}\big\{v(\tau);\quad]a,b[\,\big\}. \tag{4.21}
$$

As a consequence, we can repeat the estimate (4.20) with v in the role of u and obtain

$$
\limsup_{h\to 0+} \frac{1}{h}\int_a^b \Big|v(\tau+h,\ x) - U(\tau+h,\ x)\Big|\ dx = \mathcal{O}(1)\cdot\varepsilon. \tag{4.22}
$$

Together, (4.20) and (4.22) imply (4.12). Since $\varepsilon > 0$ and the interval $[a,b]$ were arbitrary, this achieves a proof of Theorem 6.

5 - The Glimm scheme

The fundamental paper of Glimm [18] contained the first rigorous proof of existence of global weak solutions to hyperbolic systems of conservation laws. For several years, the Glimm approximation scheme has provided the foundation for most of the theoretical results on the subject. We shall now describe this algorithm in a somewhat simplified setting, for systems where all characteristic speeds remain inside the interval $[0,1]$. This is not a restrictive assumption. Indeed, consider any hyperbolic system of the form

$$
u_t + A(u)u_x = 0,
$$

and assume that all eigenvalues of A remain inside the interval $[-M, M]$. Performing the linear change of independent variables

$$y = x + Mt, \qquad \tau = 2Mt,$$

we obtain a new system

$$u_\tau + A^*(u)u_y = 0, \qquad A^*(u) \doteq \frac{1}{2M}A(u) + \frac{1}{2}I$$

where all eigenvalues of the matrix A^* now lie inside the interval $[0,1]$.

To construct an approximate solution to the Cauchy problem

$$u_t + f(u)_x = 0, \qquad u(0,x) = \bar{u}(x), \tag{5.1}$$

we start with a grid in the t-x plane having step size $\Delta t = \Delta x$, with nodes at the points

$$P_{jk} = (t_j, x_k) \doteq (j\Delta t,\ k\Delta x) \qquad j,k \in \mathbb{Z}\,.$$

Moreover, we shall need a sequence of real numbers $\theta_1, \theta_2, \theta_3, \ldots$ *uniformly distributed* over the interval $[0,1]$. More precisely, for every $\lambda \in [0,1]$, the percentage of points θ_i, $1 \le i \le N$ which fall inside $[0,\lambda]$ should approach λ as $N \to \infty$, i.e.:

$$\lim_{N\to\infty} \frac{\#\{j\ ;\ \ 1 \le j \le N,\ \ \theta_j \in [0,\lambda]\ \}}{N} = \lambda \qquad \text{for each } \lambda \in [0,1]. \tag{5.2}$$

By $\#I$ we denote here the cardinality of a set I.

At time $t = 0$, the Glimm algorithm starts by taking an approximation of the initial data $\bar{u}$, which is constant on each interval of the form $\,]x_{k-1},\, x_k[\,$, and has jumps only at the nodal points $x_k \doteq k\,\Delta x$. To fix the ideas, we shall take

$$u(0,x) = \bar{u}(x_k) \qquad \forall x \in [x_k,\ x_{k+1}[\,. \tag{5.3}$$

For times $t > 0$ sufficiently small, the solution is then obtained by solving the Riemann problems corresponding to the jumps of the initial approximation $u(0,\cdot)$ at the nodes x_k. Since by assumption all waves speeds are contained in $[0,1]$, waves generated from different nodes remain separated at least until the time $t_1 = \Delta t$. The solution can thus be prolonged on the whole time interval $[0,\ \Delta t[$. For bigger times, waves emerging from different nodes may cross each other, and the solution would become extremely complicated. To avoid this unpleasant situation, a restarting procedure is adopted. Namely, at time $t_1 = \Delta t$ the function $u(t_1-,\cdot)$ is approximated by a new function $u(t_1+,\cdot)$ which is piecewise constant, having jumps exactly at the nodes $x_k \doteq k\,\Delta x$. Our approximate solution u can now be constructed on the further time interval $[\Delta t,\ 2\Delta t[$, again by piecing together the solutions of the various Riemann problems determined by the jumps at the nodal points x_k. At time $t_2 = 2\Delta t$, this solution is again approximated by a piecewise constant function, etc...

A key aspect of the construction is the restarting procedure. At each time $t_j \doteq j\,\Delta t$, we need to approximate $u(t_j-,\cdot)$ with a a piecewise constant function $u(t_j+,\cdot)$, having jumps precisely at the nodal points x_k. This is achieved by a random sampling technique. More precisely, we look at the number θ_j in our uniformly distributed sequence. On each interval $[x_{k-1},\,x_k[$, the old value of our solution at the intermediate point $x_k^* = \theta_1 x_k + (1-\theta_1)x_{k-1}$ becomes the new value over the whole interval:

$$u(t_j+,\ x) = u\big(t_j-,\ \theta_j x_k + (1-\theta_j)x_{k-1}\big) \qquad \forall x \in [x_{k-1},\,x_k[\,. \tag{5.4}$$

An approximate solution constructed in this way is illustrated in fig. 32. The asterisks mark the points where the function is sampled, assuming $\theta_1 = 1/2$, $\theta_2 = 1/3$.

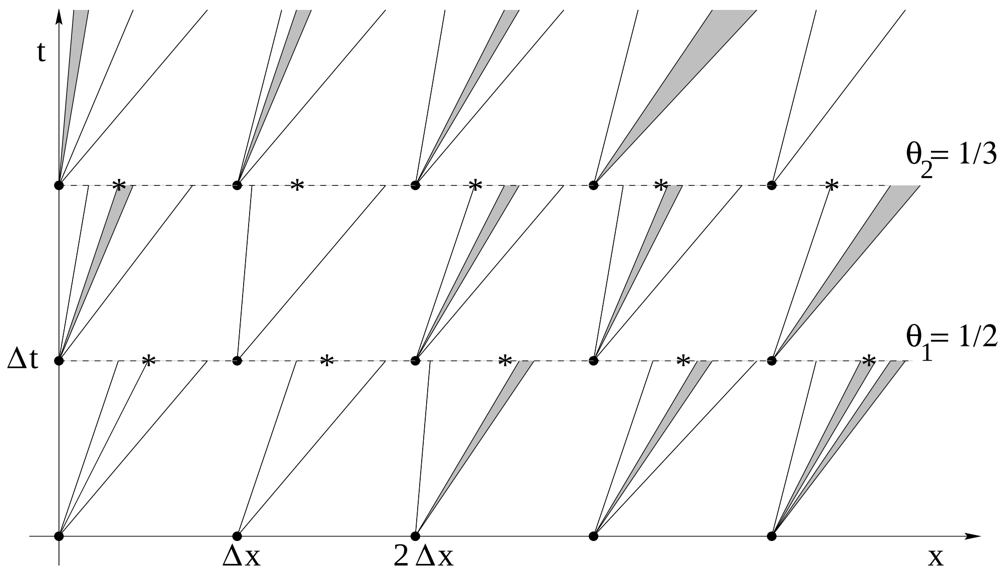

figure 32

The fundamental results of Glimm [18] and Liu [23] have established that

1. If the initial data $\bar{u}$ has small total variation, then an approximate solution can be constructed by the above algorithm for all times $t \geq 0$. The total variation of $u(t,\cdot)$ remains small.

2. Letting the grid size $\Delta t = \Delta x$ tend to zero and using always the same numbers $\theta_j \in [0,1]$, one obtains a sequence of approximate solutions u_ν. By Helly's compactness theorem, one can extract a subsequence that converges to some limit function $u = u(t,x)$ in $\mathbf{L}^1_{\text{loc}}$.

3. If the numbers θ_j are uniformly distributed over the interval $[0,1]$, i.e. if (5.2) holds, then the limit function u provides a weak solution to the Cauchy problem (5.1).

The importance of the sequence θ_j being uniformly distributed can be best appreciated in the following example.

Example 8. Consider a Cauchy problem of the form (5.1). Assume that the exact solution consists of exactly one single shock, travelling with speed $\lambda \in [0,1]$, say

$$U(t,x) = \begin{cases} u^+ & \text{if} \quad x > \lambda t, \\ u^- & \text{if} \quad x < \lambda t. \end{cases}$$

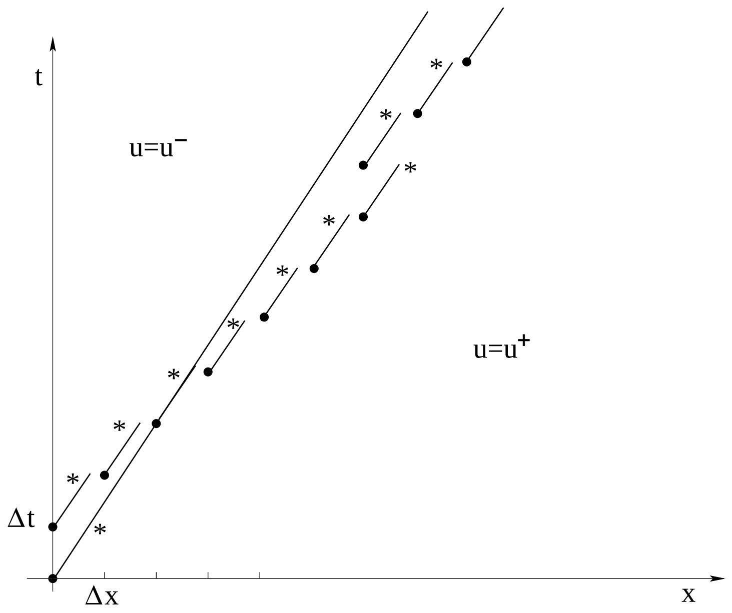

figure 33

Consider an approximation of this solution obtained by implementing the Glimm algorithm (fig. 33). By construction, at each time $t_j \doteq j\Delta t$, the position of the shock in this approximate solution must coincide with one of the nodes of the grid. Observe that, passing from t_{j-1} to t_j, the position $x(t)$ of the shock remains the same if the j-th sampling point lies on the left, while it moves forward by Δx if the j-th sampling point lies on the right. In other words,

$$x(t_j) = \begin{cases} x(t_{j-1}) & \text{if} \quad \theta_j \in \,]\lambda, 1], \\ x(t_{j-1}) + \Delta x & \text{if} \quad \theta_j \in [0, \lambda]. \end{cases} \tag{5.5}$$

Let us fix a time $T > 0$, and take $\Delta t \doteq T/N$. From (5.5) it now follows

$$\begin{aligned} x(T) &= \#\{j\,;\ \ 1 \le j \le N,\ \ \theta_j \in [0,\lambda]\ \} \cdot \Delta t \\ &= \frac{\#\{j\,;\ \ 1 \le j \le N,\ \ \theta_j \in [0,\lambda]\ \}}{N} \cdot T\,. \end{aligned}$$

It is now clear that the assumption (5.2) on the uniform distribution of the sequence $\{\theta_j\}_{j\geq 1}$ is precisely what is needed to guarantee that, as $N\to\infty$ (equivalently, as $\Delta t\to 0$), the location $x(T)$ of the shock in the approximate solution converges to the exact value λT.

Remark 2. At each restarting time t_j we need to approximate the BV function $u(t_j-,\,\cdot)$ with a new function which is piecewise constant on each interval $[x_{k-1},\ x_k[$. Instead of the sampling procedure (5.4), an alternative method consists of taking average values:

$$u(t_j+,\,x)\doteq\frac{1}{\Delta x}\int_{x_{k-1}}^{x_k}u(t_j-,\,y)\,dy\qquad\qquad \forall x\in[x_{k-1},\,x_k[\,. \tag{5.6}$$

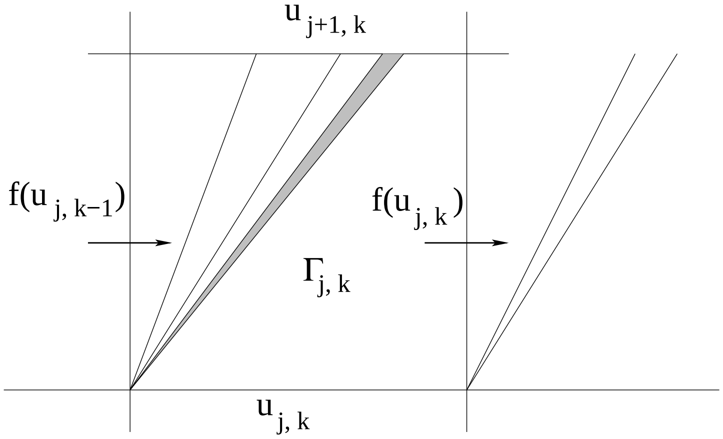

figure 34

Calling u_{jk} the constant value of $u(t_j+)$ on the interval $[x_{k-1},x_k[$, an application of the divergence theorem on the square Γ_{jk} (fig. 34) yields

$$u_{j+1,k}=u_{j,k}+\big[f(u_{j,k-1})-f(u_{j,k})\big] \tag{5.7}$$

Indeed, all wave speeds are in $[0,1]$, hence

$$u(t,x_{k-1})=u_{j,k-1},\qquad\qquad u(t,x_k)=u_{j,k}\qquad \forall t\in[t_j,t_{j+1}[\,.$$

The finite difference scheme (5.6) is the simplest version of the Godunov (upwind) scheme. It is very easy to implement numerically, since it does not require the solution of any Riemann problem. Unfortunately, it is very difficult to obtain a priori bounds on the total variation of solutions constructed by the Godunov method. Proving the convergence of these approximations remains an outstanding open problem.

The remaining part of this chapter will be concerned with error bounds, for solutions generated by the Glimm scheme.

Observe that, at each restarting time $t_j = j\,\Delta t$, the replacement of $u(t_j-)$ with the piecewise constant function $u(t_j+)$ produces an error measured by

$$\big\|u(t_j+) - u(t_j-)\big\|_{\mathbf{L}^1}$$

As the time step $\Delta t = T/N$ approaches zero, the total sum of all these errors does not converge to zero, in general. This can be easily seen in Example 8, where we have

$$\begin{aligned}\sum_{j=1}^{N} \big\|u(t_j+) - u(t_j-)\big\|_{\mathbf{L}^1} &\geq \sum_{j=1}^{N} |u^+ - u^-| \cdot \Delta t \cdot \min\big\{(1-\lambda),\ \lambda\big\}\\ &= |u^+ - u^-| \cdot T \cdot \min\big\{(1-\lambda),\ \lambda\big\}.\end{aligned}$$

This fact makes it difficult to obtain sharp error estimates for solutions generated by the Glimm scheme. Roughly speaking, the approximate solutions converge to the correct one not because the total errors become small, but because, by a sort of randomness in the sampling choice, small errors evetually cancel each other in the limit.

Clearly, the speed of convergence of the Glimm aproximate solutions as $\Delta t, \Delta x \to 0$ strongly depends on how well the sequence $\{\theta_i\}$ approximates a uniform distribution on the interval $[0,1]$. In this connection, let us introduce

Definition 3. Let a sequence of numbers $\theta_j \in [0,1]$ be given. For fixed integers $0 \leq m < n$, the *discrepancy* of the set $\{\theta_m, \ldots, \theta_{n-1}\}$ is defined as

$$D_{m,n} \doteq \sup_{\lambda\in[0,1]} \left| \lambda - \frac{\#\{j\ ;\ \ m \leq j < n,\ \ \theta_j \in [0,\lambda]\ \}}{n-m} \right|. \tag{5.8}$$

We now describe a simple method for defining the numbers θ_j, so that the corresponding discrepancies $D_{m,n}$ approach zero as $n - m \to \infty$ at a nearly optimal rate.

Fix an integer $r \geq 2$. Every integer $k \geq 1$ can then be uniquely written in base r, i.e. as a sum of powers of r of the form

$$k = k_0 + k_1 r + \ldots + k_M r^M \qquad\qquad 0 \leq k_i \leq r-1. \tag{5.9}$$

In connection with (5.9) we then define

$$\theta_k \doteq \frac{k_0}{r} + \frac{k_1}{r^2} + \ldots + \frac{k_M}{r^{M+1}}\ \in [0,1]. \tag{5.10}$$

For example, writing integer numbers in the usual basis $r = 10$, the computation of θ_k is as follows. One simply has to invert the order of the digits of k and put a zero in front:

$$\theta_1 = 0.1\,, \quad \ldots \quad , \quad \theta_{759} = 0.957\,, \quad \ldots \quad , \quad \theta_{39022} = 0.22093\,, \quad \ldots$$

For the sequence (5.9)-(5.10), one can prove that the discrepancies satisfy

$$D_{m,n} \leq C \cdot \frac{1 + \ln(n-m)}{n-m} \qquad\qquad \forall n > m \geq 0 \tag{5.11}$$

for some constant $C = C(r)$. See [12] for details. For approximate solutions constructed in terms of the above sequences (θ_j), using the restarting procedures (5.3)-(5.4), sharp error estimates can be proved.

Theorem 7. *Given any initial data $\bar{u} \in \mathbf{L}^1$ with small total variation, call $u^{\text{exact}}(t, \cdot) = S_t \bar{u}$ the exact solution of the Cauchy problem (5.1). Moreover, let $u^{\text{Glimm}}(t, \cdot)$ be the approximate solution generated by the Glimm scheme, in connection with a grid of size $\Delta t = \Delta x$ and a fixed sequence $(\theta_j)_{j \geq 0}$ satisfying (5.11). For every fixed time $T \geq 0$, letting the grid size tend to zero, one has the error estimate*

$$\lim_{\Delta x \to 0} \frac{\left\| u^{\text{Glimm}}(T, \cdot) - u^{\text{exact}}(T, \cdot) \right\|_{\mathbf{L}^1}}{\sqrt{\Delta x} \cdot |\ln \Delta x|} = 0\,. \tag{5.12}$$

In other words, the $\mathbf{L}^1$ error tends to zero faster then $\sqrt{\Delta x} \cdot |\ln \Delta x|$, i.e. slightly slower than the square root of the grid size.

To prove Theorem 7, one first constructs a front tracking approximate solution $u = u(t, x)$ that coincides with u^{Glimm} at the initial time $t = 0$ and at the terminal time $t = T$. This construction is based on a fundamental lemma of T.P.Liu [23]. The $\mathbf{L}^1$ distance between $u(T, \cdot)$ and the exact solution $S_T \bar{u}$ can then be estimated using the error formula (4.1). For all details we refer to [12].

6 - Counterexamples

In the previous chapters, the global existence and uniqueness theory for weak solutions to systems of conservation laws was developed under certain key assumptions. In particular:

- The system is strictly hyperbolic.

- The initial data is small in BV.

In this final chapter, we consider three examples showing that:

1. If the system is not strictly hyperbolic, BV solutions may not depend continuously on the initial data, in the $\mathbf{L}^1$ norm.

2. If the initial data is in $\mathbf{L}^\infty$ but with possibly unbounded variation, then the solution may become measure-valued in finite time. In such case, the uniqueness and continuous dependence of solutions may also fail.

3. If the total variation of the initial data is large, then the $\mathbf{L}^\infty$ norm of the solution may blow up in finite time. In particular, no global solution exists in BV.

Example 9. Consider the following simple model of traffic flow. Denote by x the space coordinate along a highway. Call $k(x)$ the number of lanes open to traffic. Typically, one will have $k(x) = 2$ for most x, except along some short stretches of the highway where $k(x) = 1$ because one lane is closed due to repair work. Calling $u = u(t,x)$ the density of cars (= number of cars per kilometer), we consider the system

$$\begin{cases} u_t + f(k,u)_x = 0, \\ \qquad\qquad k_t = 0, \end{cases} \qquad\qquad f(k,u) \doteq 8ku - u^2. \tag{6.1}$$

Consider first the family of stationary solutions

$$u^\varepsilon(t,x) = \begin{cases} 3 & \text{if} \quad x \in [0,\varepsilon], \\ 1 & \text{if} \quad x \notin [0,\varepsilon], \end{cases} \qquad\qquad k_\varepsilon(t,x) = \begin{cases} 1 & \text{if} \quad x \in [0,\varepsilon], \\ 2 & \text{if} \quad x \notin [0,\varepsilon], \end{cases}$$

Clearly, as $\varepsilon \to 0$, the functions $u^\varepsilon, k^\varepsilon$ converge in $\mathbf{L}^1_{\rm loc}$ to the constant solutions

$$u(t,x) \equiv 1, \qquad\qquad k(t,x) \equiv 2.$$

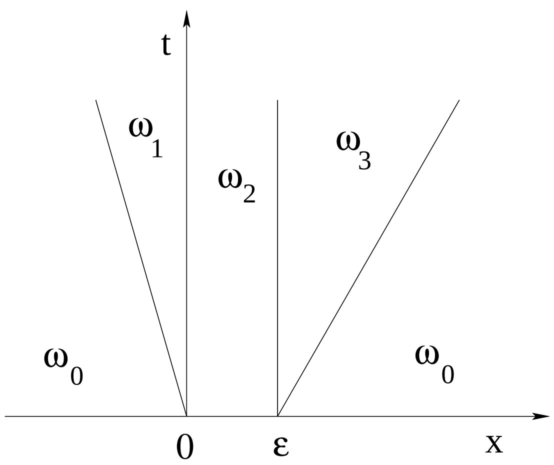

figure 35

On the other hand, consider now the family of (time-dependent) solutions (fig. 35)

$$(k^\varepsilon, u^\varepsilon)(t,x) = \begin{cases} \omega_0 & \text{if} \quad x/t < -6/(3+2\sqrt{3}), \\ \omega_1 & \text{if} \quad -6/(3+2\sqrt{3}) < x/t < 0, \\ \omega_2 & \text{if} \quad 0 < x < \varepsilon, \\ \omega_3 & \text{if} \quad 0 < (x-\varepsilon)/t < 6/(2\sqrt{3}-3), \\ \omega_0 & \text{if} \quad 6/(2\sqrt{3}-3) < (x-\varepsilon)/t, \end{cases}$$

where (fig. 36)

$$\omega_0 = (2,\,2), \qquad \omega_1 = (8+4\sqrt{3},\ 2), \qquad \omega_2 = (4,\,1), \qquad \omega_3 = (8-4\sqrt{3},\ 2).$$

Observe that, as $\varepsilon \to 0$, the initial data converges to the constant function

$$\bar{u}(x) \equiv 2, \qquad \bar{k}(x) \equiv 2.$$

However, for times $t > 0$, the solutions u^ε do not converge to the corresponding constant solution

$$u(t,x) \equiv 2, \qquad k(t,x) \equiv 2.$$

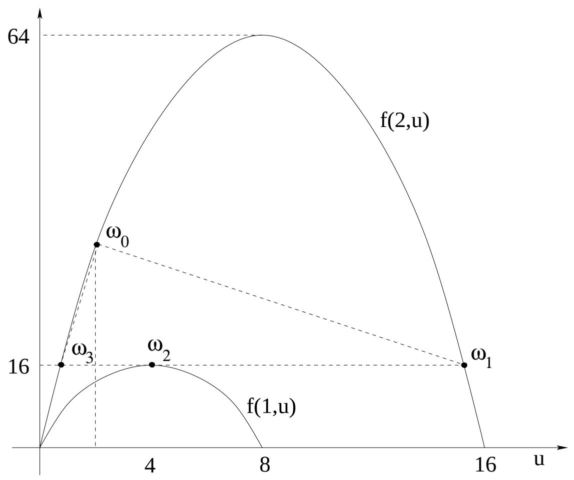

figure 36

Example 10. We now consider the Cauchy problem for a strictly hyperbolic 3×3 system of the form

$$\begin{cases} u_t + u_x = 0, \\ v_t - v_x = 0, \\ w_t + \big[\phi(u,v)\cdot w\big]_x = 0, \end{cases} \qquad \begin{cases} u(0,x) = \bar{u}(x), \\ v(0,x) = \bar{v}(x), \\ w(0,x) = \bar{w}(x). \end{cases} \tag{6.2}$$

for some smooth function $\phi : I\!R^2 \mapsto [-1/2,\ 1/2]$. Observe that the above system is strictly hyperbolic, with characteristic speeds

$$\lambda_1 = -1, \qquad \lambda_2 = \phi(u,v), \qquad \lambda_3 = 1.$$

All fields are linearly degenerate. If the initial data $\bar u, \bar v$ are in BV, then by a result in [2] it follows that the O.D.E. for characteristics

$$\dot x = \psi(t,x) \doteq \phi\big(u(t,x), v(t,x)\big) \tag{6.3}$$

has unique solutions. On the other hand, it is possible to choose $\bar u, \bar v \notin BV$ and $\phi \in \mathcal{C}^\infty$ such that the corresponding O.D.E. (6.3) has multiple (forward and backward) solutions through a given point (fig. 37). In this case, if we look at the conservation equation for w, we see that all the mass initially located within the interval $[a,b]$ will be concentrated at the single point at time τ. The $\mathbf{L}^\infty$ norm of the solution thus blows up, and the solution itself becomes measure-valued. After time τ, the solution may be prolonged as a measure-valued solution in many different ways. Indeed, the Dirac mass at P may be split among different characteristics emerging from P, or else continued as a single Dirac mass moving along any one particular characteristic originating from P.

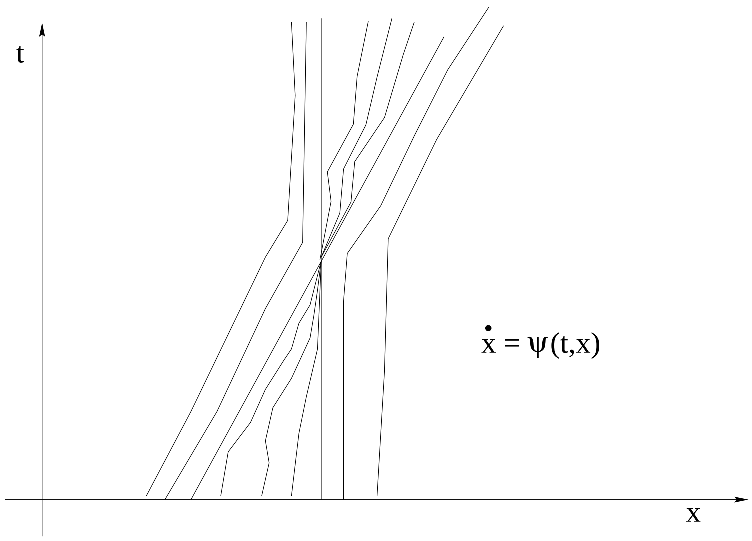

figure 37

An example where this happens is the following. Take (fig. 38)

$$\bar u(x) = \bar v(x) = \varphi(x) \doteq \begin{cases} 1 & \text{if} \quad 2^{-2n-1} < |x| < 2^{-2n} \\ -1 & \text{if} \quad 2^{-2n} < |x| < 2^{-2n+1} \end{cases}$$

$$\phi(u,v) \doteq \frac{1-uv}{6}.$$

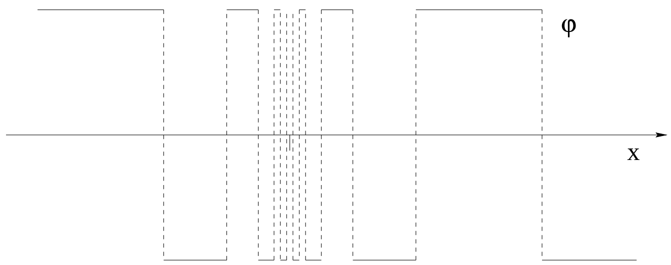

figure 38

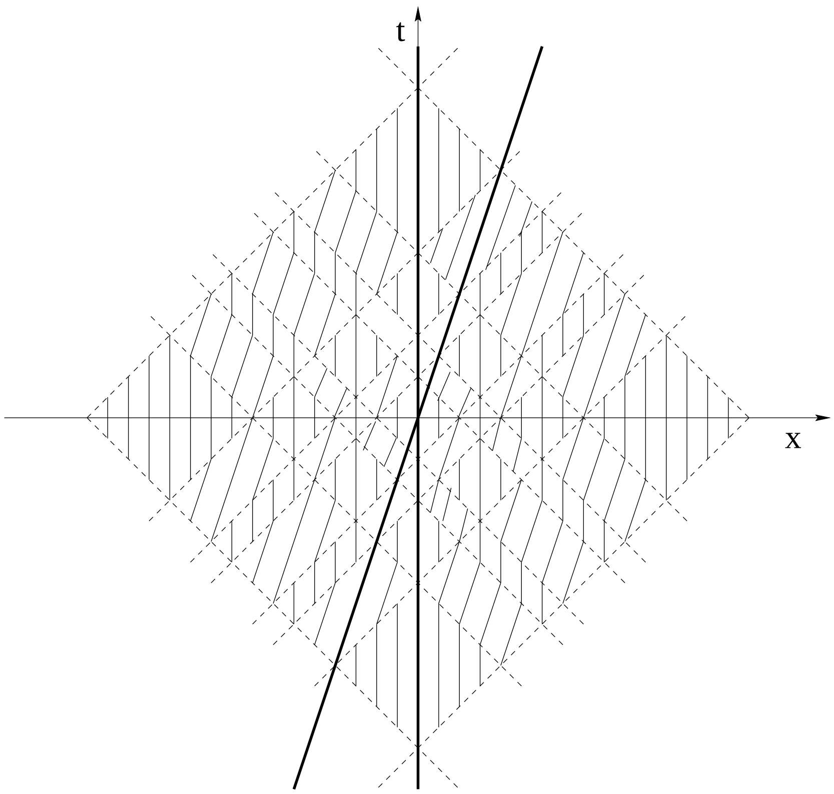

figure 39

In this case, it is easy to see that the O.D.E. (6.11) admits infinitely many solutions through the origin (fig. 39).

Example 11. Following [19], consider a 3×3 system of the form

$$U_t + F(U)_x = 0, \tag{6.4}$$

where $U = (u, v, w)$ and

$$F(U) = F(u, v, w) = \begin{pmatrix} uv + w \\ g(v) \\ u\big(1 - v^2\big) - vw \end{pmatrix}$$

We assume that the scalar function g is strictly convex, with

$$g(0) = 0, \qquad g(v) = g(-v), \qquad -1 < g'(v) < 1 \tag{6.5}$$

for all v. It is then clear that the system is strictly hyperbolic in the region where $|v| < 1$. Indeed

$$A(U) \doteq DF(u, v, w) = \begin{pmatrix} v & u & 1 \\ 0 & g'(v) & 0 \\ 1 - v^2 & 2uv - w & -v \end{pmatrix}$$

is a matrix with real distinct eigenvalues

$$\lambda_1 = -1, \qquad \lambda_2 = g'(v), \qquad \lambda_3 = 1.$$

The corresponding right eigenvectors are

$$r_1 = \begin{pmatrix} 1 \\ 0 \\ -1 - v \end{pmatrix} \qquad r_2 = \begin{pmatrix} 0 \\ 1 \\ 0 \end{pmatrix} \qquad r_3 = \begin{pmatrix} 1 \\ 0 \\ 1 - v \end{pmatrix}.$$

The first and third characteristic fields are linearly degenerate, the second is genuinely nonlinear.

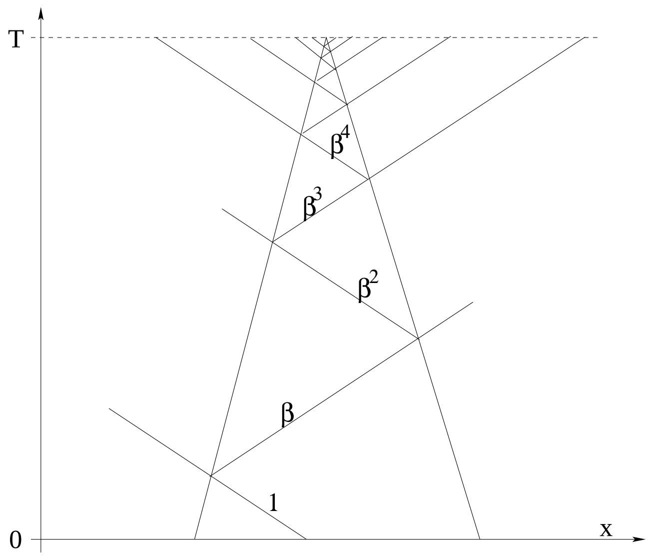

figure 40

By a suitable choice of the function g, the analysis in [19] shows that one can construct a solution $U = U(t, x)$ of the following form (fig. .40). The initial data contains two approaching 2-shocks, and a 1-wave between them, of unit strength. Subsequent interactions produce alternatively a 3-wave and a 1-wave, with strengths given as in fig. 40, with $\beta > 1$. The $\mathbf{L}^\infty$ norm of the solution, and hence also its total variation, approach infinity as $t \to T-$, the time where the two 2-shocks hit each other.

This example shows that, in general, if the initial data are large enough, the solution can blow up in finite time. For special systems, however, a global existence theorem holds also in the case of large BV data. In particular, this is true for the p-system (1.62), as proved by R. Young [30].

References

[1] P. Baiti and H. K. Jenssen, On the front tracking algorithm, *J. Math. Anal. Appl.* **217** (1998), 395-404.

[2] A.Bressan, Unique solutions for a class of discontinuous differential equations, *Proc. Amer. Math. Soc.* **104** (1988), 772-778.

[3] A. Bressan, Global solutions of systems of conservation laws by wave-front tracking, *J. Math. Anal. Appl.* **170** (1992), 414-432.

[4] A. Bressan, The unique limit of the Glimm scheme, *Arch. Rational Mech. Anal.* **130** (1995), 205-230.

[5] A. Bressan, *Hyperbolic Systems of Conservation Laws. The One Dimensional Cauchy Problem*, Oxford University Press, 2000.

[6] A. Bressan and R. M. Colombo, The semigroup generated by 2×2 conservation laws, *Arch. Rational Mech. Anal.* **133** (1995), 1-75.

[7] A. Bressan, G. Crasta, and B. Piccoli, Well posedness of the Cauchy problem for $n \times n$ systems of conservation laws, *Amer. Math. Soc. Memoir* **694** (2000).

[8] A. Bressan and P. Goatin, Oleinik type estimates and uniqueness for $n \times n$ conservation laws, *J. Differential Equations*, **156** (1999), 26-49.

[9] A. Bressan and P. LeFloch, Uniqueness of weak solutions to hyperbolic systems of conservation laws. *Arch. Rational Mech. Anal.* **140** (1997), 301-317.

[10] A. Bressan and M. Lewicka, A uniqueness condition for hyperbolic systems of conservation laws, *Discr. Con. Dynam. Syst.* **6** (2000), 673-682.

[11] A. Bressan, T. P. Liu and T. Yang, L^1 stability estimates for $n \times n$ conservation laws, *Arch. Rational Mech. Anal.* **149** (1999), 1-22.

[12] A. Bressan and A. Marson, Error bounds for a deterministic version of the Glimm scheme, *Arch. Rat. Mech. Anal.* **142** (1998), 155-176.

[13] A. Bressan and W. Shen, Uniqueness for discontinuous O.D.E. and conservation laws, *Nonlinear Analysis, T. M. A.* **34** (1998), 637-652.

[14] C. Dafermos, Polygonal approximations of solutions of the initial value problem for a conservation law, *J. Math. Anal. Appl.* **38** (1972), 33-41.

[15] C. Dafermos, *Hyperbolic Conservation Laws in Continuum Physics*, Springer-Verlag, 1999.

[16] R. J. DiPerna, Global existence of solutions to nonlinear hyperbolic systems of conservation laws, *J. Differential Equations* **20** (1976), 187-212.

[17] L. C. Evans and R. F. Gariepy, *Measure Theory and Fine Properties of Functions*, C.R.C. Press, 1992.

[18] J. Glimm, Solutions in the large for nonlinear hyperbolic systems of equations, *Comm. Pure Appl. Math.* **18** (1965), 697-715.

[19] H. K. Jenssen, Blowup for systems of conservation laws, *SIAM J. Math. Anal.* **31** (2000), 894-908.

[20] F. John, Formation of singularities in one-dimensional nonlinear wave propagation, *Comm. Pure Appl. Math.* **27** (1974), 377-405.

[21] S. Kruzhkov, First-order quasilinear equations with several space variables, *Mat. Sb.* **123** (1970), 228–255. English transl. in *Math. USSR Sb.* **10** (1970), 217–273.

[22] P. D. Lax, Hyperbolic systems of conservation laws II, *Comm. Pure Appl. Math.* **10** (1957), 537-566.

[23] T. P. Liu, The deterministic version of the Glimm scheme, *Comm. Math. Phys.* **57** (1977), 135-148.

[24] T.-P. Liu and T. Yang, L^1 stability of conservation laws with coinciding Hugoniot and char-

acteristic curves, *Indiana Univ. Math. J.* **48** (1999), 237-247.

[25] T.-P. Liu and T. Yang, L^1 stability of weak solutions for 2×2 systems of hyperbolic conservation laws, *J. Amer. Math. Soc.* **12** (1999), 729-774.

[26] N. H. Risebro, A front-tracking alternative to the random choice method, *Proc. Amer. Math. Soc.* **117** (1993), 1125-1139.

[27] D. Serre, *Systemes de Lois de Conservation I, II*, Diderot Editeur, 1996.

[28] J. Smoller, *Shock Waves and Reaction-Diffusion Equations*, Springer-Verlag, New York, 1983.

[29] A. I. Volpert, The spaces BV and quasilinear equations, *Math. USSR Sbornik* **2** (1967), 225-267.

[30] R. Young, The p-system II: The vacuum, preprint.

Several recent papers on conservation laws are also available on the preprint server http://www.math.ntnu.no/conservation/